Journal of MATERIALS RESEARCH

Invited Feature Paper-Review
DOI:10.1557/s43578-022-00524-2

EARLY CAREER SCHOLARS IN MATERIALS SCIENCE 2023

Insights of 3D bioprinting and focusing the paradigm shift towards 4D printing for biomedical applications

Kirti Agarwal[1], Varadharajan Srinivasan[2], Viney Lather[3], Deepti Pandita[4], Kirthanashri S. Vasanthan[1,a)]

[1] Amity Institute of Molecular Medicine & Stem Cell Research, (AIMMSCR), Amity University Uttar Pradesh, Sector-125, Noida 201313, India
[2] JSS Academy of Higher Education, Sector 62, Noida 201301, India
[3] Amity Institute of Pharmacy, Amity University Uttar Pradesh, Sector-125, Noida 201313, India
[4] Department of Pharmaceutics, Delhi Institute of Pharmaceutical Sciences and Research, Government of NCT of Delhi, Delhi Pharmaceutical Science and Research University, 110017, New Delhi, India
[a)] Address all correspondence to this author. e-mail: kirthanasv@gmail.com

Received: 18 November 2021; accepted: 22 February 2022; published online: 27 October 2022

Three-dimensional (3D) bioprinting is a versatile technique for biomedical applications, and includes organ printing, 3D disease model development, and drug delivery. The bioprintable materials combined with live cells have been utilized as bioinks in 3D bioprinter to fabricate versatile 3D printed structures. The 3D structures developed with smart and responsive materials can change their dimension, a technique similar to self-assembly, unfolding a new branch termed as four-dimensional (4D) printing. This manuscript reviews the details of various bioprintable materials and 3D printers, the application of 3D printing in biomedicine, smart materials, and stimulations for 4D printing. Further, this article also summarizes the regulatory issues and the limitations involved with the bioprinting. The advancements in 3D and 4D printing technology have significantly contributed to the medical field, and adequate research and amalgamation of engineering and science ideas will strengthen the application of this technology and bring solution for the existing problems.

Varadharajan Srinivasan

Varadharajan Srinivasan Dr. Varadharajan Srinivasan is currently working as Associate Professor at JSS Academy of Technical education, Noida, India. He joined the department in 2020 and is working on characterization and testing of different types of materials and industrial wastes for development of sustainable infrastructure. Dr S. Varadharajan received his Ph.D. from NIT Kurukshetra, India in 2015, where he was actively working on selection and development of eco-friendly building materials. His research interests include incorporation of latest technologies like 3D printing as a tool for development of sustainable and eco-friendly materials. In addition, the author is developing simple software tools for seismic characterization of eco-friendly building materials to cater needs of people residing in high seismic risk zones. His recent focus is on 3D material printing for various health care applications. Dr Varadharajan was the recipient of MHRD fellowship, Government of India for masters and doctoral studies from 2007-2014.

Introduction

Three-dimensional (3D) bioprinting, a highly researched and promising technology, has been exploited for various biomedical applications like regenerative medicine, implant designing, and drug delivery. The concept of printing in the manufacturing industry was introduced in the early 1950s to print various plastics, metals, glass, etc. Bioprinting was introduced in the biomedical field to print the biological components to definite

TABLE 1: Commercially available bioinks marketed by leading biotechnology-based companies.

Company	Commercial name	Material	Application
CELLINK (Sweden)	Cellink—A Cellink—[1]RGD	Alginate RGD-Alginate	Any human cells Bone & vascular implants
	Chitoink	Chitosan with glucomannan and a glycerol phosphate salt, crosslinked with [2]TPP after bioprinting	cartilage, skin, and bone
	[3,4]GelMA X series GelMA GelMA A GelMA C GelMA[7]HA GelMA Fibrin	GelMA modified with tricalcium phosphate, laminins and fibrinogen with 0.25% [5]LAP GelMA is modified with methacryloyl groups to crosslink with LAP or exposure to [6]UVLight Blend of GelMA and alginate GelMA and nanofibrillated cellulose GelMA–HA incorporates methacrylated hyaluronic acid Fibrinogen converted to fibrin is blended with GelMA	muscular contraction and neural tissue models All mammalian cells skin, cartilage, bone, connective tissue, and nerves Blood vessel
	[8]Coll 1 ColMA	Collagen type 1 methacrylated rat tail collagen 1	All types of cells
SIGMA-ALDRICH	Alginate bioink Alginate-RGD bioink	Alginate Alginate with RGD peptides	skin, bone, vascular grafts, and cartilage structures
	Cellulose–Alginate Bioinks Cellulose–Alginate–Calcium Phosphate bioink	Alginate with nanocellulose Cellulose–Alginate–Calcium Phosphate	Hard and soft tissues Skin, bone, vascular grafts, and cartilage structures
	Cellulose–Alginate–RGD bioink	alginate & nanocellulose with Arg-Gly-Asp (RGD)	Hard and soft tissues
	[9]3D printing graphene ink	Viscous liquid graphene	
	3D Printing [10]HApInk (Or)Hyper elastic bone 3D printing ink	85:15—HAp:[11]PLGA	Bone
BiogelX (United Kingdom)	BiogelX™-INKs	Synthetic peptide hydrogels	3D structures suitable for regenerative medicine and drug screening
	BiogelX™ Hydrogels	Self-assembled peptides	
	BiogelX™-INK-RGD	Fibronectin functionalized synthetic Peptide hydrogels	
	BiogelX™-INK-[12]GFOGER	Collagen functionalized synthetic Peptide hydrogels. Contains hexapeptide GFOGER	
ALLEVI (Pennsylvania, USA)	Sodium alginate	Sodium Alginate mixed with Allevi Life support	
	Liver [13]dECM	type I collagen and Xylyx Bio's highly desired liver-specific TissueSpec® [14]ECM	
	Life support	Sterile, dry, gelatin microparticles to be blended with all variants of polymers marketed by Allevi	
Bioink Solution, Inc (United Kingdom)	Gel4Cell®Kit: Gel4Cell®[15]BMP Gel4Cell®[16]VEGF Gel4Cell®[17]TGF	Gelatin-based hydrogels to be modified with growth factors	Bone tissue Vascular tissue Cartilage tissue
	PolyInks: PolyInks®-[18]PCL PolyInks®-[19]PLA	Polymeric filaments of biodegradable polymers PCL PLA	Tissue engineering & drug delivery applications
AKIRA SCIENCE (Sweden)	AKIMed-c12	Degradable filament	Tissue engineering application

TABLE 1: (continued)

Company	Commercial name	Material	Application
VivaxBio (New York, USA)	Viscoll	Viscous collagen hydrogel	All mammalian cells
SunP Biotech (New Jersey, USA)	SunP Gel G1	Gelatin methacrylate To be mixed with photoinitiator or UV cross-linked	All animal & human cells
	SunP Gel A1	Biodegradable bioink	
	SunP Gel S1	Pluronics F127-based bioink	
Advanced Biomatrix (San Diego, USA)	Lifeink® 200	Col type 1—neutral	All animal & human cells
	Lifeink® 240	Col type 1—acidic	
	Hystem®	Thiol-Modified Hyaluronan Hydrogel kit	
	PhotoCol®	Methacrylated Col type 1	mesenchymal stem cells, fibroblasts, adipose-derived stem cells, epithelial cells
	PhotoGel®	GelMA	endothelial cell morphogenesis, cardiomyocytes, epidermal tissue, bone differentiation, cartilage regeneration
	PhotoHA®	Methacrylated Hyaluronic acid	osteogenic differentiation of [20]MSC's
INNOTERE biomaterials (Radebeul Germany)	Plotter-Paste-[21]CPC	CPC paste	Bone regeneration

[1]RGD—Arginine–Glycine–Aspartate motifs; [2] TPP—tripolyphosphate; [3]Gel—gelatin; [4]Gel MA—methacrylated gelatin; [5]LAP—lithium phenyl-2,4,6 trimethyl benzoyl phosphinate, photoinitiator; [6]UV—Ultra violet light; [7]HA—hyaluronic acid; [8]Col—collagen; [9]3D—three dimensional; [10]HAp—hydroxyapetite; [11]PLGA—poly(lactic-co-glycolic) acid; [12]GPOGER—hexapeptide sequence found in collagen; [13]dECM—decellularized extracellular matrix; [14]ECM—extracellular matrix; [15]BMP—bone morphogenetic factor; [16]VEGF—vascular endothelial growth factor; [17]TGF—transforming growth factor; [18]PCL—poly(ε-caprolactone); [19]PLA—polylactic acid; [20]MSC—mesenchymal stem cells; [21]CPC—calcium phosphate cement.

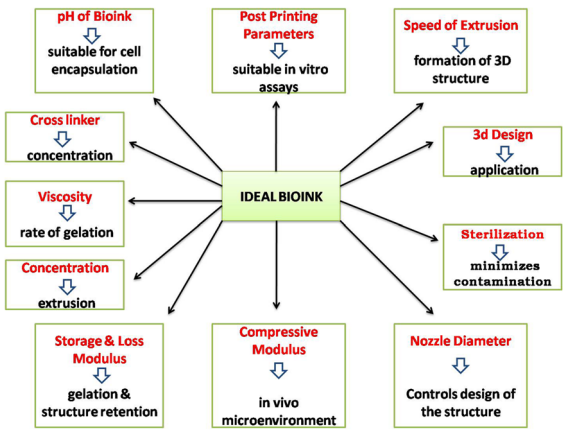

Figure 1: Various properties of ideal bioink.

design similar to their complex in vivo microenvironment to develop into functional tissue. To cater to the need of the healthcare sector, 3D bioprinting using bioinks is composed of living cells, and biocompatible material started to evolve in early 2000. Several parameters decide the process of 3D bioprinting, which includes the selection of bioink, type of bioprinter, choice organ regeneration, etc., while each factor decisively alters the target application [1].

The most crucial part of 3D bioprinting involves the bioink selection as they mediate cell orientation and cell–matrix interaction leading to organ development. Various commercial bioinks marketed by biotech companies utilize food and drug administration (FDA)-approved materials (Table 1). Since being biocompatible, these may be utilized along with desirable live cells to print 3D functional structures, and researchers have been involved in developing various bioinks to address diverse applications for biomedical applications. Figure 1 describes the ideal properties of bioink for 3D bioprinting. Variation in the concentration, ratio, and polymer type in the bioink affects the extent of gelation and rheological property that may eventually damage the printability, resulting in the rapid collapse of the 3D printed tissue. Apart from withstanding the stability, the 3D printed constructs should be biodegradable, biocompatible, and less immunogenic [2]. The prime advantage of 3D bioprinting lies in its ability to simultaneously print live cells and inks into desirable 3D structures that initiate cell–material interaction from the initial contact of the bioink. This promotes the establishment of stable cell–matrix interaction and facilitates

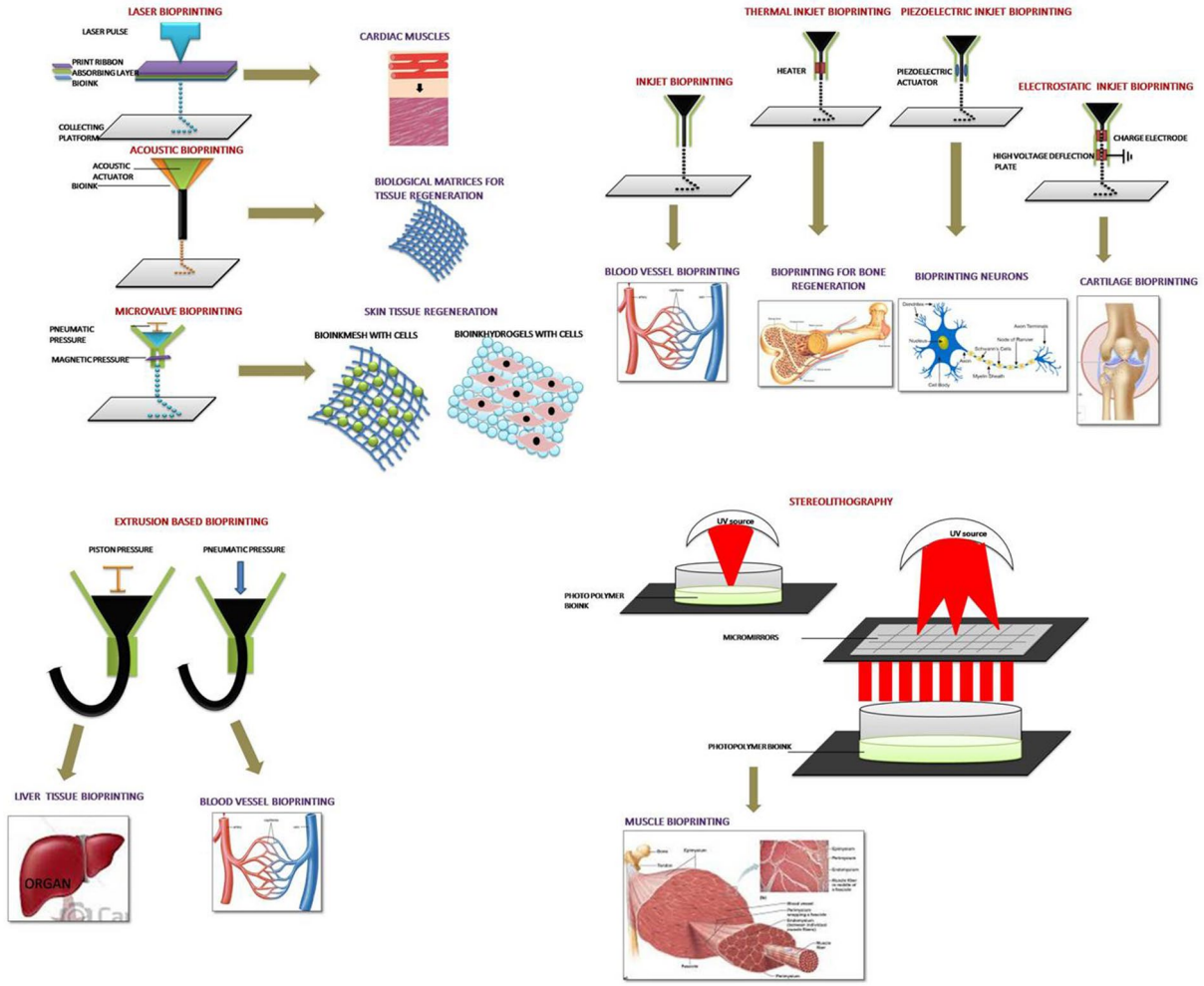

Figure 2: 3D bioprinters for various organ regeneration.

the development of the functionalized organ. Figure 2 represents the utilization of 3D bioprinters for various organ regeneration.

Besides the bioink, the type of bioprinter employed for 3D bioprinting directs the formation of 3D constructs. The in vitro 3D disease models developed via 3D printing helps to understand disease morphology and could be utilized for drug screening and minimize the use of animals as experimental models [3]. The 3D printed cancer model helps to track the disease progression and further accelerates the process of drug development. This review highlights the key aspects of 3D bioprinting including different types of bioinks and bioprinters used for organ regeneration and disease model development. The physicochemical and formulation properties of different bioinks used for bioprinting and the next-generation materials for 4D printing technology that would assist in choosing the bioinks in commercial bioprinters have been highlighted and compared in detail. Further, the shift from 3 to 4D printing for biomedical applications, which is shaping the true meaning for personalized medicine, has been reviewed.

Type of bioinks

Biomaterials employed in developing bioinks comprise natural or synthetic polymers or extracellular matrix (ECM) components [4]. The synthetic polymers possess the enhanced mechanical strength required for printing. Generally, they lack cell-responsive motifs that hinder cell attachment, proliferation, and differentiation. In contrast, most natural polymers possess favorable cell recognition motifs due to their inherent cell receptors, but limitations like biocompatibility, rapid degradation, and lack of mechanical properties need to be addressed. Thus combination, modification, and chemical structure alteration of natural/synthetic polymers supplement each other to form stable bioinks.

Prime parameters to be considered when developing bioinks include solubility, concentration, ratio, viscosity, gelation time, biocompatibility, and immunogenicity. These parameters also decide the printability, i.e., the extrusion/flow of the material from the printer nozzle. Based on the origin of polymers' origin,

inks may be categorized as natural, synthetic, and decellularized ECM (dECM) inks.

Natural polymers as inks

Gelatin

Gelatin, a thermosensitive, water-soluble protein obtained by denaturation of triple helix protein collagen I has ECM mimicking property, and its different forms have been isolated from various sources of collagen and utilized as a scaffold for tissue engineering [5]. They are biodegradable, and possess excellent biocompatibility, low antigenicity, the presence of intrinsic arginine–glycine–aspartate (RGD) motifs, efficient processing, and cellular affinity [6]. Gelatin solution forms hydrogel at low temperature (below 20 °C), during this sol–gel transition procedure (gelation), the gelatin molecules successively adjoin by non-specific electrostatic, hydrogen and hydrophobic bonds, a form of physical crosslinking to obtain 3D hydrogels, although, poor mechanical stability has been observed when the gelatin hydrogels get expose to temperature above its melting point, i.e., 28 °C [7]. The physically crosslinked bonds of gelatin molecules disorganize, followed by disintegration of the structural integrity of 3D constructs. Chemically modified hydrogels obtained by chemical crosslinking of gelatin yield a stable 3D construct to combat this problem. Various chemical crosslinking agents like genipin, glutaraldehyde, tyrosinase, and dextran dialdehyde modify and enhance gelatin's binding and gelation properties to form crosslinked hydrogels [8].

Gelatin, when blended with chitosan, alginate, fibrinogen, polyethylene glycol (PEG), hyaluronan, and methacrylamide, forms hybrid hydrogel, improves mechanical and structural stability of 3D constructs [9]. A blend of gelatin–alginate bioink encapsulated with myoblasts to investigate the mechanical properties of soft tissue constructs. By double/triple crosslinking of gelatin-based composite hydrogel, the 3D printed constructs were stabilized [10]. Kumar et al. used furfuryl-gelatin (f-gelatin) blended with hyaluronic acid (HA) to bioprint rectangular and circular structures, crosslinking of the printed structure was done by the exposure of riboflavin or rose Bengal as a visible light crosslinker and proved by Fourier-transform infrared spectroscopy (FTIR) and rheometry [11]. In an interesting study, methacrylated gelatin (GelMA) was formed by the hybridization of gelatin with methacrylamide groups followed by photo-polymerization using photoinitiator and ultra violet (UV) crosslinking. GelMA hydrogel had high cell survival capability with cell density of 1.5×10^6 cells/mL for more than eight days [12]. In another research study, a blended cell-laden bioink containing GelMA, sodium alginate, and 4-arm poly (ethylene glycol)-tetra-acrylate (PEGTA) with HUVEC and human mesenchymal stem cells (hMSC) was utilized to bioprint 3D perfusable vascular constructs with calcium chloride ($CaCl_2$) and UV crosslinking. This study highlighted suitable proliferation and spreading of the bioprinted cells [13]. From these reports, we can infer gelatin's chemical and biological ability to be used as bioinks for 3D printing.

Collagen

Collagen, an essential component of ECM, belongs to the fibrous protein family, containing a triple helical structure made up of three collagen peptides composed by repeating units of glycine–proline–hydroxyproline (GLY–X–Y). About 28 different types of collagen have been isolated from various animal and human sources, of which type I and type II collagens originate abundantly in bone, skin, tendon, and cartilage. Over the last decades, collagen fabricated into a 3D scaffold has been widely used for various tissue engineering applications as it improves cell adhesion, cell proliferation, and differentiation properties [14]. To improve viscosity and mechanical strength, alter degradation rate such that it can be developed as an ideal bioink with effective printability combination with polymers such as agarose, alginate, hyaluronic acid, fibrin, and gelatin, preferred to form the 3D structure of collagen [15]. Michael et al. utilized collagen bioink encapsulated with mouse skin fibroblast and keratinocytes for 3D bioprinting of multilayer skin tissue constructs and demonstrated that the bioprinted skin tissue constructs formed similar tissue-like skin in vivo within 11 days [16]. Lee et al. used collagen hydrogel as a scaffold material to fabricate dermal and epidermal sections of 3D skin tissue in a pattern of layer-by-layer printing of 6×6 mm collagen matrix layer, 4×4 mm keratinocytes, and fibroblasts cell layer. The study showed that 3D printed skin tissue constructs mimic the in vivo human skin [17]. In a research work, collagen–gelatin–alginate bioink with human corneal epithelial cells was utilized to bioprint cell-laden macroporous scaffold tissue constructs with the dimension of 30×30 mm in cross-section and 0.8 mm (eight layers) thickness. The bioprinted scaffold tissue constructs were incubated in sodium citrate solution to acquire degradation-controllable 3D bioprinted tissue constructs. The results demonstrated stable 3D bioprinted tissue constructs with over 90% cell viability, high proliferation rate, and cytokeratin 3 expressions [18]. Yang et al. formulated bioink using sodium alginate and collagen encapsulated with chondrocytes to bioprint 3D cartilage tissue constructs [19]. Overall, it may be inferred that when collagen are printed, it can yield stable 3D structures.

Silk

Silk fibroin (SF), fibrous protein-polymer present in the glands of arthropods such as spiders, silkworms, scorpions, bees, mites, and during their metamorphosis, gets spun into fibers [20]. The sources show variation in their structure, composition, and properties and can be further processed into several forms like particles, films, powder, sponges, fibers, and hydrogel, which can

be helpful in tissue engineering. SF protein, produced by a silkworm *Bombyx mori*, has been used for various biotechnological and biomedical applications, such as wound dressing, vascular prosthesis, enzyme immobilization matrix, drug delivery, and structural implants [21]. Silkworm silk contains 390 kDa heavy chain (H-chain), 26 kDa light chain (L-chain), and 25 kDa glycoprotein in a ratio of 6:6:1. H-chain has hydrophobic domains of repeating hexapeptide sequence of glycine-alanine-glycine-alanine-glycine-serine while the L-chain has non-repetitive amino acid sequence which makes it relatively hydrophilic and elastic [22]. With the increase in biological and clinical applications of silk, several attempts have been underway to create silk-based constructs through 3D bioprinting techniques. Inkjet bioprinting of silk-alginate as bioink crosslinked with horseradish peroxidase has been reported for fabricating soft tissue implants. Methacrylated silk (Sil-MA) has been demonstrated as an effective bioink produced by chemical modification of SF with glycidyl methacrylate (GMA), and the modification was confirmed by FTIR spectroscopy. In this study, complex organ structures were constructed, including ear auricle, cerebral sulcus, heart, lung lumen inside the trachea, and vascular network using 30% Sil-MA [21]. Admane et al. utilized SF-gelatin hydrogel and enzymatically crosslinked it with (800 units/ml) mushroom tyrosinase. About 2×10^6 cells/ml fibroblasts and 5×10^6 cells/ml keratinocytes were mixed with silk-gelatin blend bioink to bioprint 3D skin tissue scaffold with 10×10 mm size of 10 dermal layers and 8 epidermal layers as represented in Fig. 3. Results showed that the 3D bioprinted skin constructs mimic native skin tissue [23]. Sharma et al. used SF-gelatin (SF-G)-based bioink with and without $CaCl_2$. The hMSC laden SF-G and SF-G-$CaCl_2$ bioinks were used to bioprint 10-layered bone tissue scaffolds with dimensions of 5×5 mm. About 430 units of tyrosinase were added to SF-G and SF-G-$CaCl_2$ blends for enzymatic crosslinking. The study illustrated that the addition of 2.6 mM calcium ions in bioink could further enhance osteogenesis of hMSCs compared to the bioink without calcium ions [24]. Based on the evidence, SF could be confirmed as an excellent bioink choice for bioprinting.

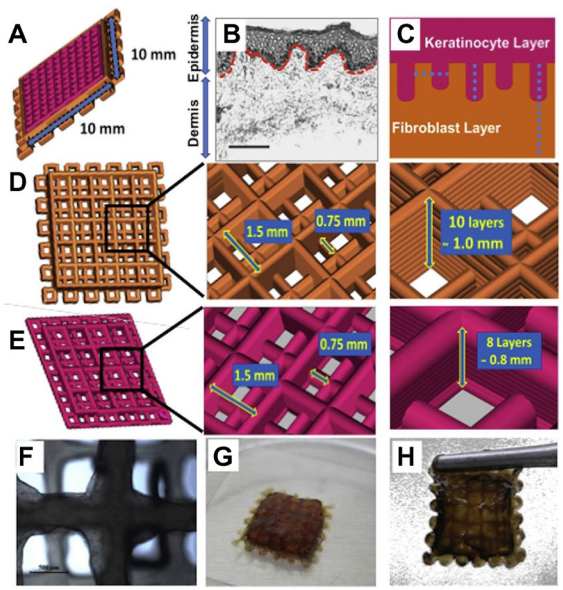

Figure 3: Schematic representation of the design strategy of the bioinspired, 3D Bioprinted construct. (A) Graphical representation of the Computer-Aided Design of the dual-layered skin model. The epidermal layer has been designed to invaginate the dermal layer at regular intervals to form rete ridges. (B) Representation of the human skin showing the dermis and epidermis. (C) Structure design strategy for the 10×10 mm, dual layered, 3D printed construct. (D and E) Detailed layer design dimensions of the dermal layer and epidermal layers, respectively. The dermal layer is constructed of 10 layers and epidermal of 8-layered filaments, arranged perpendicular to each other (in X and Y axes) with interfilament spacing of 0.75 mm and Z axis increment of 0.08 mm between each layer. (F) Microscopic image of the bioprinted construct. (G) Dual layered 1010 mm 3D printed construct in culture. (H) Mechanically stable 3D printed construct offers suitable handling properties for easy characterization [reproduced with permission from Ref. [23] copyright with license Id: 5115200903352].

Fibrin

A non-globular, blood-derived fibrous protein, fibrin, involved in the natural process of tissue repairing and blood clotting, forms by the polymerization of fibrinogen by enzymatic treatment of the protease thrombin and easily crosslinked by the incubation of fibrinogen, thrombin, and calcium ions. By mitigating or eradicating the possibilities of immunological incompatibility, fibrinogen could often be used as a scaffold material for tissue regeneration [25]. Challenges in printing fibrin-based hydrogels result from low viscosity, quick degradation velocity, rapid gelation process, and limited mechanical strength, which creates difficulty to form stable 3D constructs. To overcome these challenges, a physical blending of the fibrinogen solution with crosslinkable natural polymers, like alginate, hyaluronan, gelatin, and collagen, may circumvent the collapse of 3D printed structures and provide structural stability [26]. England and co-workers utilized fibrin with hyaluronic acid (HA) hydrogels, encapsulated with Schwann cells for 3D bioprinting followed by in vitro characterization to evaluate nerve regeneration [27]. Schöneberg et al. utilized fibrinogen and gelatin with human umbilical artery smooth muscle cells (HUVECs) to bioprint in vitro blood vessel structures with a wall thickness of 425 µm and diameter 1 mm. The fibrinogen was crosslinked using thrombin and $CaCl_2$, and the bioprinted structures showed high cell survivability of 83% and supportive vascular endothelial cadherin and collagen IV expression [28]. Wang et al. formulated a fibrin-based composite bioink consisting of fibrinogen, gelatin, HA with rat ventricular cardiomyocytes at 10×10^6 cells/ml concentration to biofabricate cardiac tissue constructs. The bioprinted construct was immersed in Dulbecco's modified minimal essential media (DMEM) containing thrombin for 20 min to crosslink the fibrin. The development of cardiac tissue construct was confirmed by

immunostaining and showed that the bioprinted constructs exhibited a response to cardiac-related drugs [29]. These results demonstrate the applications of fibrin bioinks in regeneration.

Alginate

Alginate, an anionic polysaccharide derived from seaweeds and brown algae has a composition of mannuronic acid (MA) and glucuronic acid (GA). The increased ratio of MA and GA provides stiffness to the structure and mechanical properties, while a decreased ratio of MA and GA provides flexibility to the structure [30]. Alginate hydrogels have been widely used as cell-laden bioinks in 3D bioprinting due to their biocompatibility, non-immunogenicity, less toxic nature, fast biodegradability, and crosslinking characteristics. It can be crosslinked upon addition of divalent cations like calcium, barium, strontium, etc. The alginate biopolymers have the characteristic property of entrapping water and other molecules through capillary forces and allow it to diffuse from inside-out, which makes it an ideal bioink for 3D bioprinting. Fan et al. utilized alginate-based bioinks encapsulated with bovine cartilage progenitor cells (CPCs) for printing hollow constructs. These printable vessels like microfluidic channels have been reported to be proficient in transporting nutrients, biomolecules, and oxygen through the constructs and support the cell growth [31]. To overcome these obstacles, chemical crosslinking and physical blending methods have been used for 3D bioprinting. Christensen et al. utilized sodium alginate bioink with NIH 3T3 cells for bioprinting vascular-like constructs in a 3D bioprinter using $CaCl_2$ crosslinker resulting in 90% cell viability post printing [32]. Similarly, different polymers like gelatin, polycaprolactone (PCL), hydroxyapatite (HAp), and poloxamer were combined with alginate to form several 3D printed structures like bone and cartilage [33]. In another study, alginate combined with polymers like GelMA and PEGTA for developing 3D bioprinted constructs was utilized for tissue engineering in which bioink was crosslinked with calcium ions followed by photo-crosslinking GelMA and PEGTA to acquire stable perusable vascular structures. PEGTA provides the required rheological and mechanical properties to the complex, multilayered hollow 3D constructs and this bioink combination delivered the suitable environment for the hMSCs and HUVECs [34]. These studies display that alginate-based bioinks has the potential to be the utmost preferred materials in 3D bioprinting technologies.

Hyaluronic acid-based bioinks

HA; an anionic, non-sulfated, natural glycosaminoglycan biopolymer that consists of repeating disaccharide units of N-acetyl-D-glucosamine and D-glucuronic acid and a natural ECM component has abundance in cartilages, neural, epithelial, connective tissues, and also acts as a lubricant [35]. Properties such as non-adhesiveness, biodegradability, and biocompatibility, receptor mediator cell attachment make HA find application in biomedical engineering [36]. HA has low mechanical integrity and slow gelation property like various natural polymers, which provide poor shape fidelity, thus hindering its usage in fabricating 3D structures. Various efforts have been made to enhance HA printability via blending and crosslinking for 3D bioprinting [37]. Crosslinking of HA by photochemical and physical methods has been mainly investigated, i.e., photochemically crosslinking by blending of methacrylate while physical incubation of HA solution at room temperature [38]. Recent reports of 3D bioprinting with adipose stem cells, chondrocytes, osteoblasts, and HAMA with GelMA have been reported. The blending of HA and its derivatives with photochemically crosslinked biopolymers like PEG further enhances the shape fidelity of 3D bioprinted [39]. Duan et al. bioprinted 3D heart valve conduits using bioink formulation of HAMA and GelMA hydrogels followed by 365 nm UV exposure and encapsulation of human aortic valvular interstitial cells. The results showed high cellular viability and deposition of collagen and glycosaminoglycans (GAGs) in the bioprinted heart valves [40]. Recently, hydroxyethyl acrylate and GelMA (HA-g-pHEA-GelMA) hydrogel encapsulated with mouse osteoblast cell was studied to bioprint lattice form scaffolds, which showed stable rheology properties and viable bone cells [41].

Chitosan

Chitosan (derivative of chitin), a high-molecular-weight linear polysaccharide, composed of β-(1–4) linked D-glucosamine with *N*-acetyl-D-glycosamine groups, derived from deacetylation of chitin (crustacean shells, shell of shellfish, mushroom envelopes, insect cuticles, and seafood industry wastes) [42], possess numerous important properties like antibacterial, biocompatibility, bioadsorbability, biodegradability that makes them to be employed for scaffold fabrication for skin, bone, and cartilage. Morris et al. formulated a hybrid hydrogel using chitosan and polyethylene glycol diacrylate (PEGDA) to fabricate ear-shaped scaffolds by employing stereolithography (SLA) technique. Post printing, the 3D printed ear scaffolds were seeded with hMSCs. The bioprinted ear scaffold showed 50 μm pore size and 400 kPa as elastic modulus to confirm long-term cell survivability by actin filament staining [43]. Ang et al. utilized chitosan-HAp hydrogel to fabricate square pattern scaffolds with $20 \times 20 \times 8.3$ mm dimensions. The scaffold was seeded with 2×10^5 human osteoblasts cells which showed inter-connected channel construction between the layers of the printed scaffolds [44]. Gu et al. formulated alginate, carboxymethyl chitosan

(CMC), and agarose with 5×10^6 human neural stem cells as bioink to generate 3D neural mini-scaffolds 10 mm^3 cuboidal geometry which were crosslinked with $CaCl_2$ and they demonstrated expansion and differentiation of encapsulated stem cells [45]. Alginate–chitosan, gelatin–alginate–chitosan, collagen–chitosan have been often used as bioinks for several 3D bioprinting applications and have been found to enhance the 3D printed structure.

Decellularized extracellular matrix as bioinks

In order to create a well-defined microenvironment mimicking the native in vivo topography, the use of decellularized tissue/organ has a critical role. Decellularization of the organ of choice has been carried out utilizing various methods to remove the live cells and retain the ECM framework of the organ, which consists of multiple ECM components such as collagen, GAG, elastin, collagen, and chondroitin sulfate [46]. In tissues, collagen retains the tensile strength while elastin fibers maintain the essential physiological elasticity and GAGs provide the viscoelasticity. Thus, cell attachment, proliferation, differentiation, migration, and maturation maintain ECM as the most essential element. The dECM obtained from decellularization of various human/animal tissues and organs like liver, skin, esophagus, and small intestinal submucosa has been carried out utilizing various decellularization processes with the help of chemicals like (i) acids and bases (sodium dodecyl sulfate (SDS), sodium deoxycholate); (ii) non-ionic detergent Triton X-100 and zwitter-ion3-[(3-cholamidopropyl)dimethylammonio]-1-propanesulfonate (CHAPS); (iii) chelating agents including ethylenediaminetetraacetic acid (EDTA) and ethylene glycol tetraacetic acid (EGTA); (iv) enzymes including trypsin and nucleases, and also physical parameters like variation in temperature and mechanical processes (blending or mixing) [47].

TABLE 2: List of the protocols for decellularization of organ to preserve the ECM.

Organ	Decellularization method			References
	Physical method	Chemical method	Enzymatic method	
LIVER		Livers were perfused with 0.01% [1]SDS followed by 1%Triton X-100		147
		Porcine livers were perfused with 1% SDS/ 1%Triton/ 1% [2]SDOC for 3 hours		
CARTILAGE	Auricular elastic cartilage was subjected to 12-h dry [3]FT at [4]RT followed by 12-h wet FT cyclein[5]PBS (– 20 °C)	Specimens were treated with 4% SDOC under agitation at RT for 4 h	Tissue specimens were submersed in 2% [6]DNase for 3 h; followed by 0.25% trypsin for 3 h after treatment with 2% DNase	47
HEART		Aortic valves were placed in 1% Triton X-100 with 0.02% [7]EDTA for 24 h	DNase-I, [8]RNase A together with RNase A(20 mg/ml) and DNase (0.2 mg/ml) at 37 °C under continuous shaking	47
ESOPHAGUS		esophagi were agitated in 4% [10]DEOX and 0.1% sodium azide in PBS for24 h at37°C; esophagi were placed under continuous agitation in 1% Triton X and 0.02% EDTA	followed by treatment with 1 M NaCl and 0.2 mg/mL DNase-I in PBS for 12 h; DNase-I, RNase A together with 20 mg/mL RNase A, and 0.2 mg/mL DNase-I for 72 h at 37 °C	47
		esophagus segments were subjected to [11]CHAPS buffer for 6 hours at 350 rpm followed by treated with SDS buffer for6 hours at 350 rpm		72
SKIN	The porcine skin was washed with distilled water, centrifuged at 3500 rpm for 5 min	Porcine skin was further decellularized using 0.1% SDS in 0.26% EDTA with 0.69% Tris under agitation for 6 h at37°C and 1%Triton X-100 in 0.26% EDTA with0.69% Tris for12 h at 37 °C Decellularized porcine skin was De-lipidized using 100% isopropanol for 12 h at 37 °C	The skin was exposed to0.25% trypsin under agitation for 6 h at 37 °C	49

[1]SDS—Sodium Dodecyl Sulfate; [2]SDOC—sodium deoxycholate; [3]FT—freeze thawing; [4]RT—room temperature; [5]PBS—phosphate-buffered saline; [6]DNase—deoxyribonuclease; [7]EDTA–Ethylenediaminetetraacetic acid; [8]RNase—ribonuclease; [9]Nacl—sodium chloride; [10]DEOX—deoxycholic acid; [11]CHAPS—3-[(3-cholamidopropyl) dimethylammonio]-1-propanesulfonate.

Post decellularization, the obtained ECM components further dissolved in suitable buffer solution may be used as ink for 3D printing. Table 2 represents the various protocols that have been established for the decellularization of organs. Pati et al. developed dECM from porcine cartilage, heart, and human adipose to prepare bioinks and used heart-dECM (hdECM) pre-gel to bioprint3D heart tissue analogs and successfully achieved higher cell survival rate and cell line-specific gene expression. Further, to improve the stability of 3D printed structures, PCL framework was utilized for 3D bioprinting of cartilage and adipose tissue constructs with dECM pre-gel [48]. Ali et al., formulated porcine kidney dECM-derived bioink by combining dECM and methacrylamide from kidney dECM methacrylate (KdECMMA), in which gelatin was employed due to its thermosensitive property. HA was employed to improve dispensing uniformity and glycerol to prevent nozzle clogging. The formulated KdECM-based bioink with human kidney cells was utilized at different concentrations (1%, 2% & 3% w/v) to bioprint square solid constructs of $6 \times 6 \times 1.2$ mm dimensions. The evaluation of 3D printed construct demonstrated that it exhibits characteristics of natural renal tissue and showed high cellular viability [49]. Toprakhisar et al. developed bovine tendon dECM (dtECM)-based bioink with encapsulated NIH3T3 cells to bioprint scaffold pattern by using a microcapillary-based bioprinting process. It was observed that the formulated dtECM bioink had no cytotoxic effect on bioprinted cells and the cells expressed lineage-specific morphology [50]. In another study, porcine decellularized small intestine submucosa (SIS) and collagen type I bioink with HUVECs in core area and human epithelial colorectal cells in shell area were used to bioprint human intestinal villi structure with $831.1 \pm 36.2 \times 190.9 \pm 3.9$ µm. The results demonstrated a significant cell proliferation rate and mucin17 expression [51]. Altogether, the studies depicted the establishment of cells on 3D bioprinted structure when dECM was utilized as bioinks due to the presence of ECM mimicking microenvironment.

Synthetic polymer-based bioinks

Synthetic polymers have been utilized for varied 3D bioprinting-based applications and many other FDA-approved polymers exhibit prolonged degradation, tunable mechanical property, and biocompatibility with versatile potential in biomedical applications.

Pluronic

Pluronic, a block copolymer well known as poloxamer, consists of two hydrophobic groups and a hydrophilic group that behaves as surfactant and is hence utilized in bioprinting. Owing to its ability to form self-assembling gels at room temperature and stand as solution at 10 °C, pluronics have the edge in 3D bioprinting. Moreover, it has better printability and temperature-responsive gelation property due to its broad range of sol–gel transition temperature (10–40 °C), i.e., the viscosity of pluronic fixed at both room temperature and human body temperature makes it preferable for use as bioinks. Suntornnond et al. utilized pluronic–GelMA hydrogel composite to print soft and perfusable vasculature-like constructs. Wu et al. printed microchannel utilizing pluronic in photopolymerizable polymer and developed microvascular structures [52]. Likewise, another group of researchers employed acrylated pluronic to create UV crosslinked 3D constructs, which were more stable than uncrosslinked constructs. While pluronic has been widely utilized as sacrificial bioink, its biocompatibility is not enough to support long-term cell survival, limits direct use as a reliable bioink for cell culture [53]. In an interesting study, the authors reported a strategy termed as nano-structuring, which enabled improving the biocompatibility, wherein they mixed acrylated and un-modified pluronic and then removed the un-modified molecules after UV crosslinking, which resulted in a significant increase in the survivability of the encapsulated chondrocytes for up to 2 weeks in culture due to the increased porosity [54]. In another study, the mechanical strength of the printed construct was found to be too low, which could be effectively increased by adding HAMA. These results suggested that Pluronic can be efficiently combined with several polymers and utilized for the bioprinting of various tissue constructs.

PEG-based hydrogels

PEG, a hydrophilic synthetic polymer with linear or branched structures, synthesized by ethylene oxide polymerization, and PEG and its derivatives being the most explored synthetic material for tissue engineering applications, has been fabricated into PEG-based hydrogels, PEG-diacrylate, and PEG-methacrylate widely used in extrusion-based 3Dbioprinting. PEG alone cannot shape hydrogel due to its low viscosity, making it impossible for 3Dbioprinting and requires acrylation or blending with other polymers. PEG was utilized to create tunable bioink formulations with a broad range of mechanical and rheological properties. PEG can also be utilized in a photopolymerizable form such as PEG-methacrylate (PEGMA) and PEGDA-based hydrogels were improved by linking process via light irradiation to induce hMSCs to chondrogenic differentiation. Roseti et al. developed PEGMA hydrogel that mimics the meniscus structure and to increase the structural support capability, the PEGMA hydrogel was UV crosslinked and the hMSCs were encapsulated [55]. Although PEG-based hydrogels have many advantages, they lack cell-binding domains and combine with RGD peptides to enhance cell adhesion. When blended with natural

biomaterials, PEG has been reported to improve the degradation properties of PEG-based constructs.

Poly(lactic-co-glycolic) acid (PLGA)

PLGA is a synthetic copolymer made up of linear aliphatic polyester of lactic acid (α-hydroxy propanoic acid), and FDA has approved glycolic acid (hydroxyacetic acid) for therapeutic devices owing to its biodegradability and biocompatibility. PLGA has been blended with various polymers viz. PLGA–collagen, PLGA–gelatin, PLGA–HAp, PLGA–phosphorylated chitosan, and 3D printed in multi-nozzle 3D bioprinters yielding hybrid 3D constructs with enhanced properties. In another study, PLGA–PEG microparticles were utilized with CMC or pluronic F127 to enhance their viscosity. The square-shaped bioprinted constructs matched Young's modulus of 57.3 MPa and yield stress of 1.22 MPa of human bone. The study revealed that incorporation of hMSCs produced more viscous bioink with high mechanical strength of bioprinted constructs, and release of a lysozyme protein was also sustained for 15 days [56]. Guo et al. bioprinted PLGA/dimethylsulfoxide (DMSO) scaffold with $5 \times 5 \times 2$ mm dimensions that were stretchable compared to scaffolds bioprinted without DMSO. The hMSCs seeded onto bioprinted scaffolds showed no cytotoxic effect after evaporation of DMSO. Further, the cell-seeded scaffolds were cultured in lineage-specific growth factors up to 21 days, which upregulated expression levels of osteogenic, chondrogenic, and adipogenic markers [57].

Poly(ε-caprolactone) (PCL)

PCL, a bioresorbable, hydrophobic, synthetic polymer, comprises excellent viscoelastic and rheological properties. It has been extensively used in tissue engineering due to its high mechanical strength, low melting point (– 60 °C), biocompatibility, biodegradability, and thermoplastic nature [58]. Chen et al. used polydopamine-modified calcium silicate (PDACS)/PCL with Wharton's jelly MSC and HUVEC for bioprinting. In this study, a PDACS/PCL hydrogel framework was printed, and then alginate–gelatin encapsulated HUVEC cells were printed between the pores of the framework, followed by printing of Wharton's jelly MSC over the PDACS/PCL scaffold, and this sequential dispensing was repeated to bioprint 16 layered hard-tissue scaffolds. The bioprinted scaffold yielded a high Young's modulus with cell growth promotion and showed a high level of angiogenic biomarkers (Fig. 4) [59]. Visser et al., in their study, showed that PCL microfiber scaffolds serve as a reinforcing element to GelMA–HA hydrogel by fabricating PCL-based soft porous microfiber scaffolds with dimension $120 \times 120 \times 1$ mm through electrospinning which also supports human chondrocytes growth [60]. In another study, PCL scaffolds measuring 10 mm diameter and 1.5 mm height were constructed with different mean pore sizes of 215, 320, 515 μm by fused deposition modeling. Among the pore sizes studied, 215 μm PCL scaffold was reported to increase rabbit BMSCs and showed better chondroprotection effect in vivo for 12 weeks in rabbits with meniscectomy [61].

Polyurethane (PU)

PU, a thermo-responsive, synthetic polymer made up of organic units joined by carbamate (urethane) links, can be either biodegradable or non-biodegradable and has been extensively used for biomedical applications viz. fabrication of intravenous perfusion tubes, inert artificial heart, the printing of nerve, muscle, and bone tissue, etc., owing to its excellent physical and bioinert properties. Merceron et al. used a 3D integrated organ printing system to bioprint muscle–tendon construct by depositing four different components. The authors co-printed mouse myoblast cell line with PU hydrogel for muscle growth and elasticity, while NIH 3T3 cells were co-printed with PCL hydrogel for providing stiffness and tendon growth. The results demonstrated elasticity on PU-myoblasts muscle side while stiffness on PCL-fibroblasts tendon side with more than 80% cell viability at day 1 and 7 post printing [62]. Hsieh et al., in their study, utilized PU hydrogel encapsulated with 4×10^6 cells murine neural stem cells (NSCs) to bioprint NSC-laden PU construct with $1.5 \times 1.5 \times 0.15$ mm dimension. In vivo implantation of 3D bioprinted construct into neural-injury model rescued adult zebrafish from traumatic brain injury [63]. Lin and colleagues, in their study, mixed soy protein isolate (SPI) with PU to improve the structural integrity of bioprinted PU–SPI hybrid construct having the dimension of $20 \times 20 \times 10$ mm. The PU–SPI bioink was blended with mouse fibroblasts and NSCs and printed at 37 °C. The embedded cells were analyzed for their viability, proliferation, and gene expressions which demonstrated better survivability and a significant increase in expression levels of neuronal-related markers like β-tubulin, nestin, microtubule-associated protein 2, and glial fibrillary acidic protein at 72 h [64].

Poly(vinyl alcohol) (PVA)

PVA, a water-soluble, linear synthetic polymer, produced by vinyl acetate polymerization, makes an excellent material for biomedical applications due to its low protein adsorption tendency, low toxicity, biocompatibility, good mechanical strength, and water retention property. Zou et al. bioprinted a microfluid channelized valentine-shaped heart using PVA as a sacrificial material extruded from the first nozzle. Alginate, agarose, platelet-rich plasma hybrid bioink with embryonic rat cardiomyocytes, and HUVEC cells were deposited in the second nozzle's internal part of the sacrificial scaffold. In vitro rheological and biological characterization of 3D printed construct showed mechanical integrity

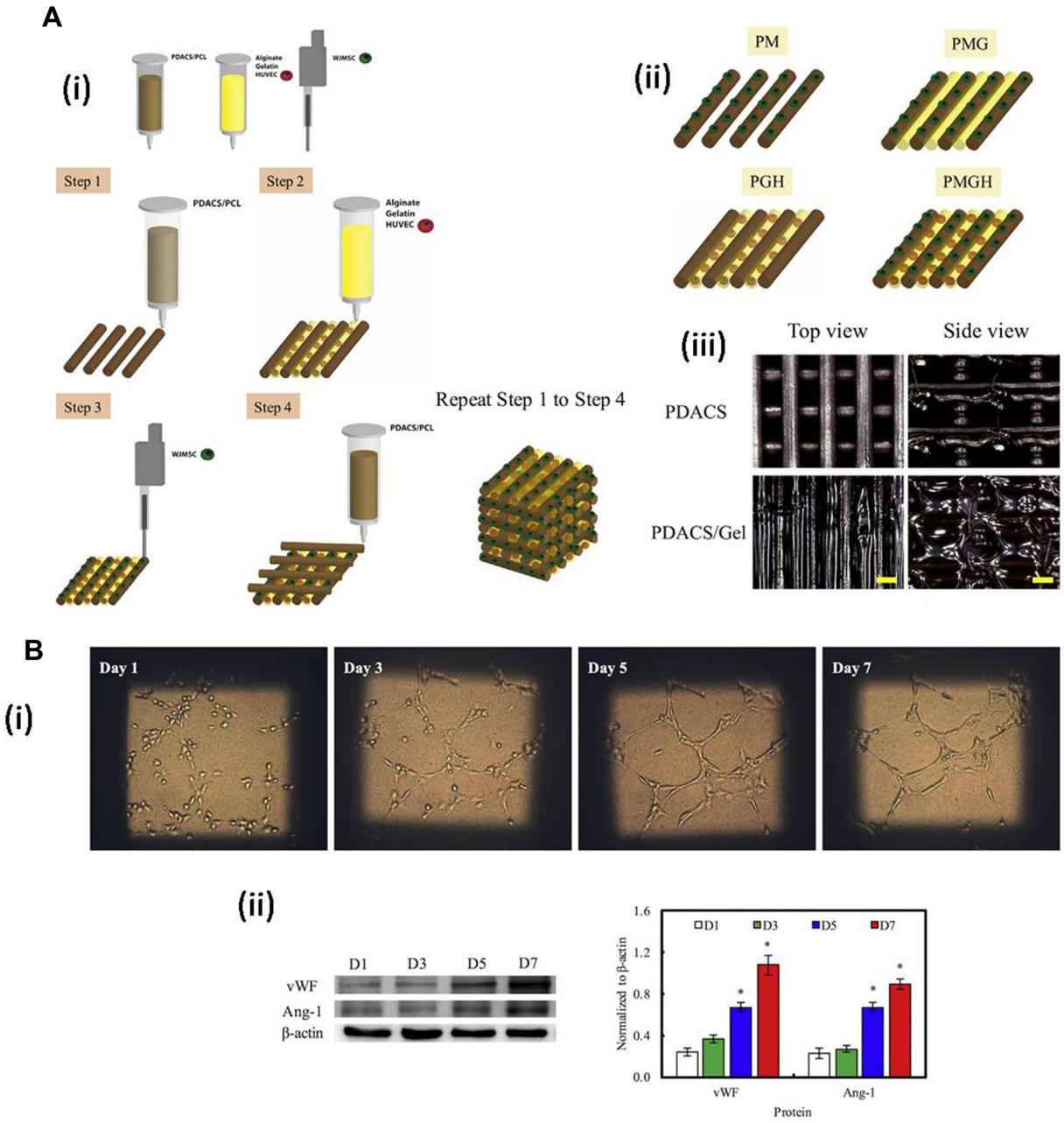

Figure 4: (a) Schematic diagram of (i) bioprinting process. First, a framework was fabricated with PDACS/PCL composite to support the entire mechanical stability. Second, the alginate/gelatin hydrogels-encapsulated HUVECs were dispensed into the pores. The WJMSCs were printed on the PDASC/PCL scaffold with the piezoelectric needle. The sequential dispensing of PDACS/PCL composite, hydrogel, and cells was repeated and stacked to build the 3D scaffold (10 layer). (ii) PM, PMG, PGH, and PMGH groups. (iii) The microstructure images of PDACS/PCL and PDACS/PCL/Gel scaffolds. (b) Proliferation of HUVEC leading to tube formation, (ii & iii) the expression levels of the angiogenic markers (vWF and Ang-1) of HUVEC in the alginate/gelatin hydrogels for 1, 3, 5, and 7 days were evaluated by Western blot analysis "*" indicates a significant difference ($P < 0.05$) from Day1. [reproduced with permission from Ref. [59] copyright with license Id: 5115340351318].

and significant cell viability and proliferation. Further, they constructed a simplified aortic valve and anatomic heart that demonstrated good elasticity and no collapse. They also performed a perfusion test through the channels of printed constructs which showed smooth perfusion of red dye solution within the fluid channels [65]. In another study, PVA-MA/GelMA blend hydrogel was used to fabricate various 3D structures (cube, pyramid, cone, flower with channels, woven mats, ring mails, 3D lattice, and gyroid structure) via digital light processing (DLP) technique. Tris-bipyridylruthenium hexahydrate and sodium persulfate were used as the photo-initiators for hydrogel crosslinking, which maintains

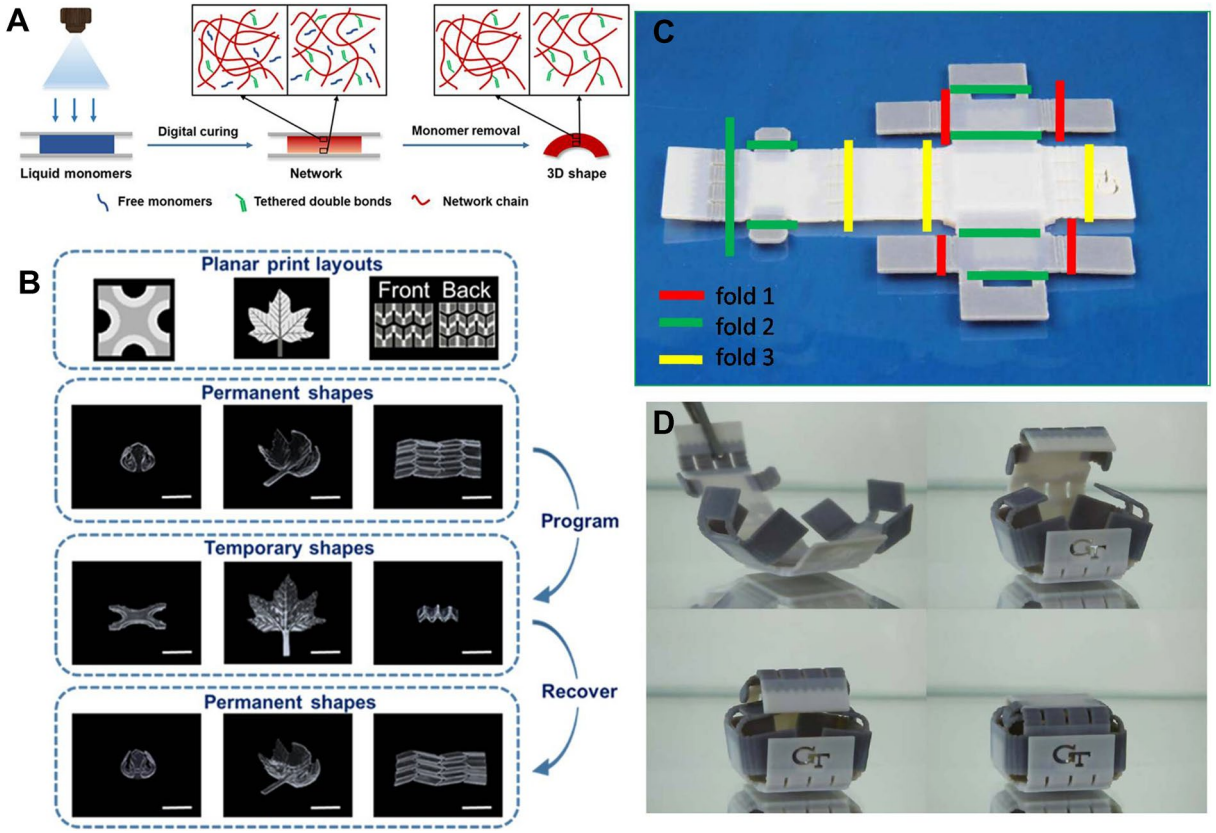

Figure 5: Fabrication of digital Shape Memory Polyurethanes (a) Schematic illustration of the fabrication process, (b) Evaluation of shape memory behavior—Digital fabrication of complex permanent shapes and demonstration of their shape memory behavior. In the planar print layouts, the black background represents no light exposure and the light and dark regions correspond to light exposure of 14 and 30 s, respectively. All scale bars are 1 cm, reproduced with permission from Ref. [146] copyright © 2019, American Chemical Society], (c) The image of 3D printed self-folding box that combined different materials at different hinges, (d) The schematic diagram of a self-locking with a different external environments upon heating [reproduced from Ref. [147] open access Scientific reports].

the mechanical integrity of the printed construct. Human endothelial colony-forming progenitor cells and hMSCs were seeded on the printed hydrogels, which confirmed the formation of osteogenic and chondrogenic tissue after 14 days of culture of stem cells post printing [66]. Yu et al. utilized alginate–PEGDA–PVA hybrid hydrogel to bioprint square geometry scaffold of $10 \times 10 \times 1$ mm size with different filament distances, i.e., 800, 1000, 1200, 1400 μm. Mouse osteoblast cells were seeded on the printed scaffolds, and in vitro evaluation of cytocompatibility and printability reported remarkable improvement in mechanical strength, cell viability, and printability with the use of PVA [67].

Smart materials for 4D printing

Various stimuli that help transform 3D to 4D printed structures include physical, chemical, and biological stimuli. Physical stimuli include temperature, photo, magneto, and electric fields of stimulation that cause the shape shifting of smart polymers. The pH response and ionic concentration makes up the chemical stimuli and is being explored for drug delivery systems. Figure 5 schematically represents the role of smart polymers and details of stimuli-responsive polymer are discussed below:

Temperature-responsive polymers

Poly(*N*-isopropylacrylamide) (PNIPAM), (poly(*N*-vinylcaprolactam), gelatin and GelMA, collagen and ColMA, methylcellulose, agarose, pluronic, and poly(ethylene glycol)-based block polymers have been investigated as temperature-responsive polymers [68]. These polymers utilize the principle of glass transition upon heating and, when cooled down, change to metastable state further modified via transformation energy.

Magnetoresponsive polymers

Iron (III)oxide (Fe3O4), mesoporous bioactive glass, PCL nanoparticles, iron(III) oxide/PCL, and iron (III)oxide/poly(ethylene glycol diacrylate) (PEGDA) nanocomposite, and PCL/iron-doped HAp (PCL/FeHA) nanocomposite respond to magnetic stimuli [69]. The iron oxide-based

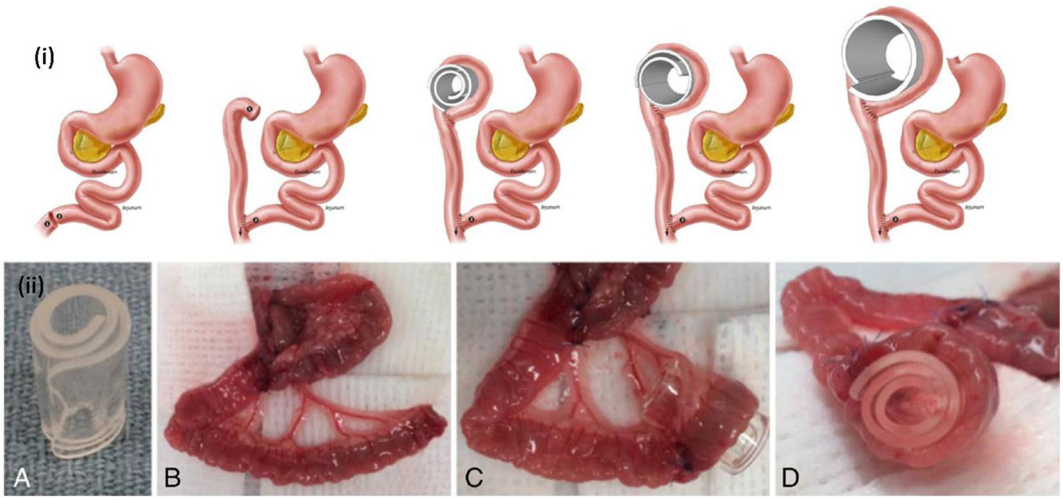

Figure 6: (i) Schematic for experimental animals; creation of Roux-en-Y limb, placement of cylindrical coil and radial expansion (over 7 days). (ii) Photographs at operation showing (A) radial expanding shape memory polymer device, (B) placed with end of Roux limb, (C) wrapped around it, (D) Control group placement of a non-expanding polymer coil. [reproduced from Ref. [148] copyright with license Id: 5115370941361].

nanoparticles with PCL have been explored in drug delivery and theragnostics applications. These smart polymers recover the shape because of heating and magnetic field and alternating magnetic field to hold the transformed shape. Figure 6 depicts the surgery on human for enterogenesis using the shape memory polymers isobornyl acrylate, 2-hydroxyethyl-acrylate, and 1,6-hexanediol diacrylate. This simple operative approach can be used to elongate intestine and grow new tissue.

Electric field-responsive polymer

Graphene-incorporated multilayer methacrylated poly(trimethylene carbonate), polyethylenimine. Use of these polymers and other biomaterials increases the electrical conductivity similar to native tissues of muscles and bone that help in the regeneration. This property can be used by neural regeneration, where the electric field guides the alignment of cells.

pH-responsive polymer

Poly(L-glutamic acid (PGA), poly(histidine) (PHIS), poly(acrylic acid) (PAA), and poly(aspartic acid) (PASA), highly researched pH-responsive polymers, change their form in response to environmental pH due to their protonation of ionizable groups and cleavage of bonds [70]. The change in pH leads to the structural transformation of these polymers due to the forces of attraction or repulsion. These properties could be best applied for enteric-coated drug delivery systems where drug delivery accelerates or hinders gastrointestinal system's pH changes. They also hold a quite promising role as gene delivery system.

Photoresponsive polymer

PNIPAM functionalized with spirobenzopyran, 4,4′-azodibenzoic acid (ADA), a-cyclodextrin, and dodecyl (C-12)-modified PAA were studied, the presence of photosensitive side chains on the polymers causes reversible or irreversible changes affecting the polarity, hydrophilicity, bond strength, etc. These have been explored for drug delivery systems where degradation of the carrier material is often dealt with this mechanism [71].

For 4D printing, utilization of the smart polymers and 3D printing systems like SLA, extrusion, FDM, photolithography-based bioprinters with external stimuli like humidity, and light and magnetic fields have been explored to develop tissue patterns. Stem cells, generally preferred cells of choice, help to differentiate to other lineages [72]. Various applications have been reported using 4D printing with smart materials; e.g., PNIPAM and PCL were electrospun into square-shaped fibrous mat and cultured mouse fibroblast cells. Upon stimulus with varying temperature, the square-shaped mat underwent self-assembly to different shapes without compromising the decline in cell number [73]. Growth factor-encapsulated PCL shape memory porous (SMP) structures were 3D printed and implanted in mandibular bone defect model rabbit. The SMP responded to body temperature, released growth factor, and recovered the SMP structure to match the defect area. This study highlights the feasibility of implanting 3D structures produced by 4D printing for drug delivery and regenerative medicine application [74].

However, to meet the challenges in 4D printing, integration of material science, biological system, and engineering aspects could form the key to address any limitation or to clear roadblocks, and exploitation of biocompatible smart polymers might speed up the process. This would benefit different branches of biomedical

sciences in areas like tissue regeneration, medical device fabrication, drug delivery, medical diagnosis, deposition of therapeutics in printlet manufacturing, and sensing applications.

Bioprinters

Bioprinters are described as robotically automated machine moves in X–Y–Z axis with the commands directed by computer-aided design (CAD) software program to fabricate the desired 3D structures being explored for various biomedical applications.

History and working principle of 3D bioprinters

The historic innovation of developing 3D bioprinters dates back to 1984, when Charles Hull, the father of 3D printing, invented the first 3Dprinter. By early 2000, the 3D printers were employed in the medical field, and in 2006, 3D in vitro human bladder was fabricated, followed by developing in vitro human veins in 2009. Several research works were started on creating in vitro ears, windpipes, veins, bones, tissues, and basic organs by 3D bioprinting technology. A typical 3D printer follows a standard series of steps to print the 3D structure, i.e., (i) *3D imaging*: to get the specific elements of the tissue, a standard CT or MRI check is used. 3D imaging ought to give an ideal mimic of the tissue with almost no alteration required with respect to the specialist; (ii) *3D Modeling*: a diagram is created utilizing AutoCAD software. The outline likewise incorporates layer-by-layer guidance in high details. Fine changes might be made at this phase to stay away from the exchange of deformities; (iii) *Bioink Preparation:* living cells along with support material similar to collagen, gelatin, HA, or nanocellulose forms bioink. During 3D printing, bioinks deposit layer by layer at a defined thickness to maximize cellular interaction; (iv) *Solidification:* viscous bioink hardens to hold its shape upon post-printing. This occurs as more layers ceaselessly deposit and crosslink.

Types of 3D printing

Commercially available bioprinters vary in operation to dispense the ink for printing and may be chosen based on the application.

Droplet-based bioprinting (DBB)

DBB, a high-resolution bioprinting technique that ejects the bioinks as droplets and deposits over a substrate, may be further classified into inkjet bioprinting, acoustic/ultrasound bioprinting, microvalve bioprinting, and electro-hydrodynamic jetting.

Inkjet bioprinting

Inkjet bioprinting, one of the oldest forms of bioprinting technology, utilizes cell-laden bioink cartridges, and further classified into two groups; continuous inkjet (CIJ) bioprinting which ejects an uninterrupted trace of bioinks through a nozzle, and drop-on-demand (DOD) inkjet bioprinting, promising over CIJ bioprinting due to its precise control over the positioning and ejection of droplets on demand. Inkjet bioprinter contains single/multiple print-heads, which consists of fluid tanks and nozzles [75]. Based on their mechanism of trigger, various types of DOD inkjet bioprinters have been used for bioprinting.

The electrostatic DOD These inkjet bioprinters produce droplets by rise in temperature between the charge electrode and high voltage deflection plate. This leads to an increase in pressure, and the bioink chamber's relative volume increases, forcing the bioink droplets out of the nozzle. In the absence of charge, high voltage deflected pressure plate regains its original form. Electrostatic DOD have high resolution and low-cost printing techniques because they are driven by electrostatic forces [76].

Thermal inkjet bioprinting This bioprinter comprises thermal actuators that, upon application of voltage pulse, heats the bioink to form bubble, which ejects out from the nozzle to the desired substrate [77].

Piezoelectric inkjet bioprinting This type of bioprinting involves bioink vaporization into bubbles by utilizing a piezoelectric actuator. Next, to develop acoustic waves inside the bioink reservoir, an attached voltage pulse causes the expansion and contraction of piezoelectric actuator that creates pressure for the ejection of bioink droplets from the printer nozzle. However, caution needs to be taken as the high frequency (15–25 kHz) of the piezoelectric actuator could lyse or harm the cell membrane of the bioink [78].

The DOD inkjet bioprinting has shown high cell viability of 80% with high resolution (~ 50 μm), and has been widely used to bioprint various organs and tissues like bone, cartilage, skin, cardiac, and nervous tissue [79]. Further, this technique requires less viscous bioink ranging from 3–12 MPa/s to avoid clogging at the nozzle orifice. In a study, bovine aortic endothelial cells, human amniotic fluid-derived stem cells, and canine smooth muscle cells were bioprinted separately utilizing a thermal inkjet bioprinter. The cells were mixed with $CaCl_2$ cross linker and deposited in a layer-by-layer pattern to bioprint sodium alginate–collagen scaffold, the 3D bioprinted construct showed vascularization when implanted in vivo [80].

Acoustic/ultrasound bioprinting

This type of drop-on-demand, orifice-free bioprinting technique employs acoustic/ultrasound waves to produce droplets from the cell-laden bioink. The bioprinting system comprises

an acoustic actuator and piezoelectric substrate on which conducting interface mainly has gold rings positioned. When the acoustic actuator starts, the surface acoustic/ultrasound waves with circular geometry are generated which forms an acoustic focal point between the ink–air interfaces at the exit of fluidic channel. This overpowers the surface tension of the bioink and ejects on the substrate [81]. It has the most significant advantage of being a nozzle-free technique and thus no effects on the printability with respect to factors like high voltage, heat, high pressure, and shear stress. This technique also offers a high printing speed of 10,000droplets/s with higher resolution (~ 37 μm) and has been reported to bioprint highly viscous bioinks with cell viability of 90%, however, it forges with a constraint that high-intensity acoustic waves may damage the cells.

Microvalve-based bioprinting

The microvalve DOD bioprinter entails a magnetized electromechanical or solenoid valve coil and an iron plunger that controls the nozzle orifice for the ejection of cell-laden bioink droplets. Multiple microvalve print-heads individually connected to gas regulator help to deliver pneumatic pressure and control the opening time of valve by the movement of the solenoid coil and iron plunger. In this printing technique, the droplets formed upon application of the electromechanical valve regulate the pneumatic switch. The working principle of the microvalve bioprinter depends upon the voltage pulse applied to create a magnetic field to pull the iron plunger upwards in ascending motion. This, in turn, unblocks the nozzle and the pneumatic pressure pushes the ink out from the nozzle [82].

Microvalve bioprinting has been consistently used to bioprint 3D tissue constructs such as skin, liver, and lung using several cell lines including smooth muscle cells, keratinocytes, fibroblasts cells, and epithelial cells [83]. Microvalve-based bioprinting has been successful due to its large nozzle diameter that reduces the shear stress of the cells, but in smaller nozzle orifice of 100–250 μm it has demonstrated clogging due to viscosity of bioinks (– 200 MPa/s). Lee et al. utilized electromechanical microvalve bioprinter to fabricate perfusable vascular channels with HUVECs (1×10^6 cells/mL) and normal human lung fibroblasts (2×10^6 cells/mL) mixed with fibrinogen and thrombin as bioink [84].

Electrohydrodynamic (EHD) jet-based bioprinting

This printer ejects bioink as droplets by utilizing a high electric field ranging from 0.5 to 20 kV, applied between the positively charged metallic needle and negatively charged substrate. Deposition of the bioink droplet from the nozzle achieved by generating repulsive coulombic force, overpowers the viscoelastic force of bioink and surface tension at the tip of the nozzle. EHD jetting can be operated in two different modes, firstly the pulsating droplets generate droplets by applying a low electric field and slowing the flow rate, and continuous stream mode results in bioink spun upon adjusting the voltage to its critical value [85]. There are various advantages of EHD jet-based bioprinting, viz., it provides higher nanoscale resolution of 100 nm and utilization of viscous bioinks of 20% w/v for bioprinting. Nevertheless, the application of a high electric field can lead to cell death, and thus its utilization for 3D organ regeneration makes it dubious [86]. Bioprinting of vascularized structures, mouse fibroblasts cells, nerve tubes, etc., using EHD jet-based bioprinters has been studied. For instance, Vijayavenkataraman et al. reported bioprinting of nerve guide conduits (NGCs) utilizing in-house built EHD jet-based bioprinter. PCL was used to print 3D scaffolds rolled into tube shape with a diameter of 1.2 ± 0.15 mm, followed by sealing of the ends with heat. About 1×10^5 cells derived from a pheochromocytoma of rat adrenal medulla were seeded over PCL scaffolds. The 3D printed tubular scaffolds were cultured up to 6–7 days followed by in vitro bioprinted tissue assessment. The results showed an optimum NGC construct with more than 60% porosity and printed scaffolds expressed β-3 tubulin and neurofilament 200 [87].

Extrusion-based bioprinting (EBB)

Extrusion-based bioprinting, also termed bioplotting or direct ink writing, has been the most extensively used modality among all bioprinting techniques. In this technique, bioink directly extrudes as continuous stream (not as droplets) from syringe nozzle using pneumatic pressure via gas or an air pump or through mechanical force by using piston or screw plunger onto a substrate by layer-by-layer fashion, as it constructs 3D structures [88]. EBB system comprises an automated robotic platform, a single or multiple printing heads movable in x, y, z axis by means of controller. Basic printing parameters such as printing speed, nozzle diameter, temperature, bioink viscosity, and extrusion pressure need to be optimized before printing. Based on the actuating modes, micro-extrusion bioprinting system divides into three types discussed in further sections.

Pneumatic-based extrusion system This technique utilizes compressed gas or air to dispense the bioink from the nozzle of the syringe. The compressed air from the air pump reaches the syringe via a connector. To minimize the contamination of bioinks and the bioprinted structures, the air pump, syringes, nozzle, connector, and collecting substrate must be sterilized [89].

Piston-based extrusion system This type, driven by mechanical force and more suitable for extruding high vis-

cous bioinks, delivers better flow than the pneumatic-driven system. Micro-infusion motor used in this technique has piston connected by means of guide screw that helps the piston to extrude the bioink out of the nozzle over the substrate [72].

Screw-based extrusion Driven by mechanical force, screw-based extrusion provides improved spatial, volumetric control, higher resolution, better printability, and can dispense highly viscous bioinks. However, this technique may harm the cells loaded in the bioink due to the presence of screw and also has issues with screw cleaning and disinfection [90]. The main advantages of EBB include better printability with highly viscous bioinks (– 600 kPa/s), compatibility with crosslinkers, scalability, fast printing speed, etc. However, it also has various limitations such as low resolution (– 100 µm), nozzle clogging; shear stress that might reduce the cell viability. The 3D bioprinting of several types of tissues and organs such as skin, liver, cardiac patch, muscle, neural tissue, bone, and cartilage, with the encapsulation of diverse cell types has been reported by utilizing EBB. Ji et al. used a bioink composed of methacrylate alginate or Me-HA and encapsulated hMSCs to create a perfusable channel by employing EBB technique [91]. Raveendran et al. utilized a micro-extrusion bioprinter to fabricate 3D scaffolds of human primary periodontal ligament cells with GelMA hydrogel. The results demonstrated that different printing parameters such as UV exposure, pressure, photoinitiator concentration, and needle diameter highly influenced the printed structure [92].

Laser-based bioprinting (LBB)

LBB, a nozzle-free, contact-less printing technique, utilizes high-power laser pulses to shape the cell-laden bioinks into 3D structural form. It works on the principle of laser-induced forward transfer (LIFT) technique for bioprinting, comprising long-wavelength pulsating laser beam, laser transparent ribbon donor slide, laser energy absorbing layer (gold, titanium, platinum), a layer containing cell-laden bioink, and a collector slide [93]. For bioprinting through laser technique, a focused high-power laser pulse directed on the ribbon stimulates the laser absorbing sacrificial layer and vaporizes the donor layer at the focused site, followed by producing a high-pressure bubble at the edge of the cell-laden bioink layer that finally propels the bioink to fall in the droplet form to the collecting slide. The resolution of laser-printed 3D structure could be influenced by the type of laser beam, surface tension, the gap between donor and receiving slide, viscosity, and thickness of donor layer and substrate wettability [94]. LBB possesses numerous exceptional advantages like it provides higher cell viability (– 95%), no nozzle clogging, exceptional resolution (> 20 µm), printing at high cell density (~ 108cells/ml), and use of bioink with 1–300 MPa/s viscosity [93]. Although an expensive technique, laser exposure may cause harm to the cells. LBB has been consistently utilized for bioprinting of bone, skin, muscles, blood vessels, adipose, cardiac tissue, cell printing, etc.

Stereolithography (SLA)

SLA, an optical-based nozzle-less additive manufacturing technique, was established in the late 1980s and utilizes spatially controlled laser (UV or visible range) to crosslink cell-laden photopolymer bioink. In this technique, a digital light projector having UV, infrared, or visible light directed on the liquid photocurable resin solidifies in a layer-by-layer pattern forming a 3D structure and the unpolymerized precursor removed from the final construct [95]. This bioprinting system eliminates the shear stress factor and offers high cell viability (more than 85%), rapid and precise fabrication process with high (100 µm) resolution. The variant of SLA includes DLP, which utilizes an array of digital micro mirror devices to project the light in a three-dimensional pattern that polymerizes the entire resin layer. Recently, advancement in SLA printing technique was reported as continuous liquid interface production that offers better resolution and improved printing speed [96]. Bioprinting of various tissues such as blood vessels, osteochondral scaffold, neuron, liver, cardiac, and cartilage using SLA has been reported. For example, Yu et al. utilized in-house rapid DLP-based 3D bioprinter to fabricate heart and liver tissue construct using porcine heart dECM (HdECM) and liver dECM (LdECM) blended with GelMA and encapsulated hiPSC-derived cardiomyocytes and hepatocytes [98]. The SLS technique may offer superior features, though potential bioinks for this technique remain a challenge.

Applications of 3D bioprinting for organ regeneration

The biochemical cues provided by bioink and the desired shape developed by 3D bioprinter offers precise microenvironment for the cell proliferation and maturation. This principle utilized for tissue and organ engineering develops accurate scaffold for various organ regeneration. Various organs regenerated with the use of bioinks have been discussed in the below sections. Table 3 highlights the commonly used bioinks for various organ regeneration.

Vascular tissue

A functional 3D bioprinted organ depends on its vascularization as it supports the diffusion of the nutrients and exchanges of gases to the cells for maintaining their functionality and survivability. This requires the presence of hollow structure in 3D structure and hence sacrificial materials like pluronic, agarose,

TABLE 3: Bioinks and bioprinters employed for organ printing.

Biomaterial	Crosslinker	Cells	Bioprinter	Organ/tissue	Dimension	In vitro/In vivo testing	References
Sodium alginate	Ionic crosslinker: [1]CaCl, [2]$CaSO_4$, and [3]$CaCO_3$	[4]MSCs	[5]3DBioplotter		printed using 25 [6]G needle, feed rate: 8 mm/s; fiber spacing: 4 mm; 0/90° pattern	Bioink printability, Cell viability, mechanical properties	147
Alginate–[7]PEG–Fibrinogen	[8]UV crosslinking	[9]HUVECs [10]iPSC-[11]CMs	[12]MPH	Cardiac tissue		Immunofluorescence [13]RT-PCR, [14] FACS	148
[15]GelMA	[16]$NaIO_4$	[17]HCASMCs HUVECs [18]hMSCs	[19]EBB	vascular	printing speed:100 mm/s; extrusion flow rate: 1.0 mL/s	Fluorescent Imaging, RT-PCR in vivo *implantation* immune fluorescence	56
[20]SF	[21]PPY, [22]Hcl, iron chloride	Schwann cells	[23]SLA-based 3D bioprinter (Regenovo, Hangzhou, China)	Neural tissue	nozzle diameter: 0.26 mm	Characterization of PPY/SF scaffolds, cell proliferation, immune cytochemistry	57
[24]HA-SH/ [25]HA-MA hydrogel	[26]I-2959, UV	[27]HDF	3D Bioplotter (Envision Tec, Gladbeck, Germany)	Skin tissue	Nozzle Diameter: 400 µm, print pressure: 1.8–2.2 bar, printing speed: 3–5 mm/s, temperature: 23 °C	morphology, swelling test, in vitro degradation cytotoxicity, in vitro drug release	58
[28]PCL–HA		[29]TGFβ3	Bioplotter (Envision Tec, Gladbeck, Germany)	Articular cartilage	bioscaffold measuring 12·42 × 10·11x 16·88 mm^3	Histology & Histomorphometric analysis, immune fluorescence, mechanical properties	58
[30]GelMA/ gellan gum		Chondrocytes	BioScaffolder dispensing system (SYS + ENG, Salzgitter-Bad, Germany)	cartilage	23G metal needle, syringe temperature was varied from 37 °C to 15 °C	Mechanical evaluation, histology, and [31] IHC, construct stiffness, biochemical assays	59
Chitosan\ HA\Collagen	Tyrosinase, [32]STPP	Fibroblasts	3D bioplotter (Envision TEC, Germany)	skin constructs	–	Histology, mechanical strength analysis, degradation rate	4
nano-ink (i.e., nHA + TGF-β1 [39]PLGA nanosphere + [40]PEG-[41]PEGDA hydrogel)	laser exposure	hMSCs	table top SLA	Osteochondrocytes	15 × 1.2 mm solid disks, layer thickness of 400 µm, in-fill density (40%, 60%, & 80%)	TGF-β1 release profile, mechanical testing, hMSC In vitro studies	59
dECM and Pluronic F127	incubation for 30–60 min at 37 °C	HDF-n, [42]HA-VSMCs, HUVECs	custom-built EBB	Arteriovenous structures	3 mL syringe with a tapered 150-µm steel & plastic needle	Rheological characterization, Fluorescent imaging	

TABLE 3: (continued)

Biomaterial	Crosslinker	Cells	Bioprinter	Organ/tissue	Dimension	In vitro/In vivo testing	References
collagen, alginate, and fibrin	gelatin slurry support bath	[43]C2C12 and [44]MC3T3	Syringe EBB 3D printer (Printrbot Jr, movie S10)	femur, branched coronary arteries, trabeculated embryonic heart, and human brain	Femur length: 35 mm; diameter: 2 mm; coronary artery wall thickness:1 mm; length:4.5 cm, lumen diameters of 1—3 mm; diameter embryonic heart 2.5 cm	tensile testing, fluorescent imaging	60

[1]$Cacl_2$—calcium chloride; [2]$CaSO_4$—calcium sulfate; [3]$CaCO_3$—calcium carbonate; [4]MSC—mesenchymal stem cells; [5]3D—three dimensional, [6]G—gauge; [7] PEG—polyethylene glycol; [8]UV—Ultra violet light; [9]HUVEC—human umbilical cord vascular endothelial cells; [10]iPSC—induced pluripotent stem cells; [11]CM—cardiomyocytes; [12]MPH—micro fluidic printing head; [13]RT-PCR—reverse transcription polymerized chain reaction; [14]FACS—Fluorescence activated cell sorting; [15]Gel MA—methacrylated gelatin; [16]$NaIO_4$—sodium periodate; [17]HCASM—human coronary artery smooth muscle cells; [18]hMSC—human mesenchymal stem cells; [19]EBB—extrusion-based bioprinter; [20]SF—silk fibroin; [21]PPY—pyrrole; [22]Hcl—hydrochloric acid; [23]SLA—stereolithography; [24]HA—hyaluronic acid; [25]HA-MA—methacrylated hyaluronic acid; [26]I-2959—Igracure photoinitiator; [27]HDF—human dermal fibroblast; [28]PCL—poly(ε-caprolactone); [29]TGF β—transforming growth factor β; [30]Gel MA—methacrylated gelatin; [31]IHC—immunohistochemistry; [32]STPP—sodium tripolyphosphate; [33]dECM—decellularized extracellular matrix; [34]LAP—lithium phenyl-2,4,6 trimethyl benzoyl phosphinate, photoinitiator; [35]hiHEP—human-induced hepatocytes; [36]DLP—digital light processing; [37]hdECM—heart decellularized extracellular matrix; [38]EHT—engineered heart tissue; [39]PLGA—Poly(lactic-co-glycolic) acid; [40]PEG—Poly(lactic-co-glycolic) acid; [41]PEGDA—polyethylene glycol diacrylate; [42]HA-VSMC—Human vascular smooth muscle cell line; [43]C2C12—mouse myoblast cell line; [44]MC3T3—mouse osteoblast cell line.

and gelatin may be utilized. Hydrogels of GelMA, dECM, alginate, collagen, PEG, etc., or their blends have been preferably utilized as bioinks to print 3D vascular tissue [94]. Zhang et al. used sodium alginate and chitosan blend bioink to bioprint tubular constructs by means of co-axial extrusion-based bioprinter. During the bioprinting process, crosslinker was ejected by contacting the bioink that resulted in rapid gelation of the bioink and formed tubular constructs [98]. Schöneberg et al. formulated two types of bioinks, i.e., gelatin with HUVECs and fibrinogen with SMCs to bioprint in vitro blood vessel construct by employing drop-based bioprinter to mimic native vascular channel [99]. Nishiyama et al. deposited 1% sodium alginate with HeLa cells crosslinked with $CaCl_2$ to fabricate cell-laden tubular structures using inkjet bioprinter [100]. Bourget et al. co-printed HUVECs and human bone marrow-derived MSCs onto a collagen biopaper by utilizing laser-assisted bioprinting technique for vascularization. Bioprinted HUVECs spread all over the collagen matrix after 24 h, while the bioprinted MSCs showed minor migration in the collagen matrix, which suggested that the endothelial cells could develop capillaries in time due to the stability of MSCs on capillaries [101].

Bone-like structures

Currently, for treating injuries related to bone, grafts like artificial implants that can withstand the compression pressure have been implanted in the defective area but may pose problems related to biocompatibility. 3D bioprinting of bone-like structures has been promising as they are patient-specific, and the 3D printed structure fits well in the defective regions. Various natural and synthetic polymer-based hydrogels with bone precursor stem cells and osteogenic lineage cells have been explored for bone tissue engineering. In a research study, alginates with polylactic acid (PLA) were used to print 3D bone tissue construct [102]. Additionally, the use of HAp, nano silicate clay, etc., offers high mechanical strength and provides stability to the structure [103]. Gao et al., in their study, utilized PEGDMA hydrogel, bioactive glass nanoparticles with hMSCs, and HAp in a thermal jet-based bioprinter to study osteogenesis [104]. Byambaa et al. used GelMA with HUVECs and hMSCs to fabricate micro-structured bone-like tissue structures comprising a perfusable vascular lumen using extrusion-based bioprinting technique. The bioprinted structure showed stability for 21 days in vitro [105]. Wenz et al. used GelMA and HAMA hydrogels modified with HAp particles and encapsulated with primary human adipose-derived stem cells (hASCs) to bioprint bone matrix with edge length of 10 mm utilizing micro-extrusion bioprinting technique [106]. Keriquel et al. used nano-HAp (nHA)–collagen hydrogel with mouse mesenchymal stromal cells to bioprint a ring with 3 and 2 mm external and internal diameters, respectively, and a disc with 2 mm diameter by using the LIFT method. The results illustrated marginal bone regeneration in-ring geometry while a significant new bone formation was seen with the disc geometry on a calvarial defect mice model [107].

Cartilage

Cartilage tissue has poor self-repair capacity and the highly prevalent disease condition involving cartilage include

osteoarthritis (degenerative joint disease), which affects millions of people worldwide. 3Dbioprinting of cartilage that mimics the native cartilage tissues has great potential in osteoarthritis treatment. Being avascular tissue with low cellular density acts as an additional advantage to 3D bioprint cartilage tissue effortlessly [108]. Natural polymers like HAp, alginate, chitosan, and collagen were investigated as blends with synthetic polymers like PCL and PGA, etc., to increase the compressive strength of the bioprinted structures [109]. Gruene et al. used LIFT technique to bioprint porcine bone marrow-derived MSCs which successfully differentiated into chondrogenic and osteogenic lineages [110]. In a most recent study, Xu et al. utilized a hybrid bioprinting method to fabricate PCL fibers by electrospinning and collagen-fibrin hydrogel encapsulated with rabbit chondrocytes was bioprinted by inkjet bioprinter [111]. Rhee et al. utilized concentrated collagen hydrogel to increase the shape fidelity with bovine meniscal fibrochondrocytes at cell density of 10×10^6 cells/ml to bioprint meniscus tissue using a commercially available 3D printer and reported 90% cell viability ten days post printing [112]. These studies show the promising effect of 3Dbioprintingwhen utilized along with chondrocytes and suitable biomaterials.

Cardiac tissues

Cardiac diseases account to be the leading cause of morbidity and mortality worldwide, with the complications arising from cardiovascular disorders being dealt with biodegradable stents and patches. Tissue-engineered 3D cardiac patches help to restore the damaged myocardium in the case of cardiac arrest [113]. For in vitro testing, reports suggest HUVEC to be the best-preferred choice of cells cultured on the 3D printed structure to assess the function of cardiac tissues. Jakab et al., in their study, employed EBB to fabricate tissue spheroids comprising HUVECs and chicken embryos myocardial tube-derived cardiac cells on a collagen biopaper in a monolayer grid pattern. Later the tissue spheroids were fused, followed by the formation of a single cardiac patch that can beat synchronously [114]. Maiullari et al. utilized alginate and PEG-fibrinogen-based bioink comprising HUVECs and iPSC-derived cardiomyocytes (iPSC-CMs) to bioprint multicellular 3D constructs of co-axial extrusion bioprinter [115]. In another research study, a blend of GelMA, alginate, and photoinitiator Irgacure 2959 seeded with HUVECs and neonatal rat cardiomyocytes was used to fabricate 3D endothelialized myocardium tissue scaffolds with dimension $5.5 \times 3.5 \times 0.75$ mm using commercial 3D bioprinter NovoGen MMX by Organovo [116]. Yu et al. reported bioprinting of striated heart and lobular liver tissue construct with dimensions measuring $3 \times 3 \times 0.25$ mm through DLP-based 3D bioprinter, using porcine HdECM, LdECM blended with GelMA, and lithium phenyl-2,4,6 trimethyl benzoyl phosphinate (LAP) photoinitiator. The hiPSCs were differentiated into cardiomyocytes and hepatocytes before combining with their respective dECM bioinks. The authors demonstrated that tissue-specific dECM bioinks offered a favorable environment for high cell viability and maturation of hiPSC-derived cardiomyocytes and hepatocytes [97].

Liver tissues

The liver has a unique self-regenerating and restoring capability, but for the patients suffering from end-stage of liver disease, orthotopic liver transplantation remains the only clinically approved treatment. 3D bioprinting provides an alternative strategy for developing liver tissue to be utilized for regeneration and drug testing. The naturally derived polymers like dECM, silk, gelatin, alginate, and synthetic pluronics constitute highly preferred biomaterials for liver tissue engineering [117]. Kim et al., in their research, bioprinted 3D liver tissue construct with the help of EBB by utilizing 3% w/v alginate polymer with 4×10^7 cells/ml suspended primary hepatocytes cells derived from 6–8-week-old mice livers. Results showed the cell viability up to 14 days with upregulated liver-specific markers like hepatocyte nuclear factor 4 alpha (HNF-4α), albumin, etc. [118]. In another study, sodium alginate hydrogel encapsulated with hiPSCs bioink was bioprinted with inkjet bioprinter to fabricate 40 layered mini-liver, which showed excellent cell viability, differentiation of hiPSCs into hepatocytes in 17 days with upregulated hepatic markers [119]. Recently, a 3D liver tissue construct with the assembled primary hepatocytes (1×10^4 cells/ml) in the spheroid form was successfully bioprinted, metabolically active for 60 days. Wu et al. bioprinted liver-mimetic honeycomb 3D construct using sodium alginate and cellulose nanocrystals along with human hepatoma cells and fibroblast cells by EBB. The bioprinted 3D constructs were crosslinked in $CaCl_2$ for 10 min and cultured in complete DMEM for 3 days which demonstrated minimal cell damage [120].

Skin tissues

Skin, the largest organ in the human body, has the self-repairing mechanism against minor injuries but cannot withstand severe damage like burns and deep wound infection, etc. Bioprinted skin promises to solve the gaps to address damages caused by larger wounds. Koch and his co-workers developed bioinks utilizing mouse fibroblast, HaCaT, and hMSCs at a density of $1–2 \times 10^6$ cells/ml resuspended in a 30 µl alginate and blood plasma. The bioinks were printed employing LIFT bioprinting technique to a chess-board pattern with 9.6×9.6 mm. In vitro tests for cell proliferation, apoptosis, and DNA damage were carried out and the results demonstrated ~ 90% cell survivability and increased cell proliferation capacity [121]. Lee et al.

employed bioprinting of collagen with human fibroblasts and keratinocytes at cell density of 1×10^6 cells/mL and printed a 10-layered square-planar construct using a microvalve bioprinter. To test the potential of multilayered cell construct, non-planar poly(dimethylsiloxane) (PDMS) mold was fabricated to create a 3D skin wound model. Results showed high cell viability and proliferation capacity on square-planar and non-planar surfaces [122]. Yanez et al. bioprinted skin grafts of $2 \times 4.5 \times 0.1$ cm dimension by utilizing inkjet bioprinter with collagen and neonatal human dermal fibroblast (NHDF) at the bottom layer. The middle layer constituted fibrin-thrombin and human dermal microvascular endothelial cells (HMVECs), and top layer consisting of collagen with neonatal human epidermal keratinocytes (NHEK). The bioprinted skin grafts were placed on the dorsal area of the wound-created mice and compared with commercial skin tissue substitutes. Results demonstrated improvement in wound contraction by 10% compared to the control groups [123]. Pourch et al. bioprinted skin construct with $1 \times 1 \times 0.5$ cm dimension utilizing blend of 10% w/v gelatin, 0.5% w/v alginate, and 2% w/v fibrinogen bioink encapsulated with 1×10^6 cells/ml mouse fibroblasts. Next, the bioprinted skin construct was seeded with NHDF cells and characterization, which demonstrated features of native human skin at molecular and macromolecular levels after 26 days of seeding [124].

Collectively, these studies emphasize the promising potential of 3D bioprinting technology to develop functional 3D structures best suitable for medical and regenerative medicine.

3D printing for disease models

3D cancer/tumor models

3D cancer/tumor models have been of substantial advantage in recapitulating the cancer cells in the desired microenvironment, and success in precisely tracing the different types of cancer cells and micro-capillaries with the help of 3D bioprinting has also been made possible. It is indeed a new technique in the gigantic field of cancer research and requires additional focus in the development of suitable 3D models [125]. Xu and colleagues studied 3D bioprinting by utilizing human ovarian cancer cells and fibroblasts cells to freely bioprint multiple cell types on a Matrigel™ in the form of multicellular acini by dual-ejector-inkjet bioprinter [126].

For cervical tumor study, Sun et al. used HeLa cells with gelatin–alginate–fibrinogen hydrogel and bioprinted to patterned shape using extrusion-based bioprinter to create in vitro cervical tumor model. By 5–8 days, HeLa cells showed more than 90% cell survivability with migration and formed cell aggregates surrounded by hydrogel fibers which demonstrated the metastasis of cancer cells [127]. In another study, cancerous HeLa cells and non-cancerous murine fibroblasts cells in PEGDA hydrogel were bioprinted with a microvascular network containing different channel widths of 25 mm, 45 mm, and 120 mm to signify diameters of blood vessels using digital micromirror device-based projection printing (DMD-PP). The authors reported that non-cancerous bioprinted fibroblasts cells remained unaffected by the different channel diameters, while the HeLa cells migrated considerably when channel diameters were decreased [128]. Dai et al. bioprinted a brain tumor model using glioma stem cells with alginate–gelatin–fibrinogen in EBB and showed in vitro temozolomide drug susceptibility of the brain tumor models [129]. Further, 3D breast tumor models were constructed by Swaminathan et al. explained that alginate hydrogel containing breast epithelial spheroids bioink were more resilient to paclitaxel than singly bioprinted breast cells [130]. Although various cancer/tumor model studies demonstrating the 3D bioprinting of tumor spheroids have been reported, more investigations warrant exemplifying the mechanistic behavior of cells with ECM to develop a stable tumor model.

Disease models

3D bioprinting enables the construction of complex functional 3D tissue models with potential use in testing, screening, and implantation of various complex tissue models and diseases (including liver, cardiac, skin, neurons). In heart disease model study, the cardiac patch was bioprinted using 3D bioplotter and bioink comprised decellularized cardiac ECM hydrogel, GelMA hydrogel, and human cardiac progenitor cells (hCPCs). It showed that utilizing GelMA–cECM in cardiac patch bioprinting resulted in 30 times of significant increase in hCPCs cardiogenic gene expression and 2-folds higher angiogenic potential as compared to GelMA alone. The bioprinted patch of dimension 10 mm × 0.6 μm was placed in vivo over the right ventricle of rat heart and vascularization was observed in 14 days [131]. In another study, a Hap-collagen-chitosan (Hap-Col1-Cs) hydrogel was utilized to fabricate biocompatible porous scaffolds by thermally induced phase separation method for restoration of maxillofacial mandible bone in the defected model. The scaffolds were processed with 2-hydroxyethyl methacrylate (HEMA) and glutaraldehyde to create Col1-Cs-HEMA and Ha-Col1-Cs-GTA chemically crosslinked scaffolds, respectively. Human amniotic fluid-derived MSCs were seeded on the fabricated scaffolds and in vitro observation showed that Hap-Col1-Cs-DHT and Hap-Col1-Cs-IR scaffolds were biocompatible non-cytotoxic for MSC proliferation. Further, Hap-Col1-Cs-DHT and Hap-Col1-Cs-IR scaffolds were surgically grafted in maxillofacial mandible bone defect rabbit models that resulted in restoration of mandible bone [132]. Gaebel et al., in their study, applied the LIFT bioprinting technique to fabricate polyester urethane urea (PEUU) cardiac patch seeded with HUVECs and hMSCs for cardiac regeneration. The synthesized patch with the thickness and diameter of 300 μm and

8 mm, respectively, possessed 91% porosity with 91 µm average pore size. The HUVECs with cell density of 4×10^6 were bioprinted onto the patch in two layers with 900 µm grid line space followed by printing of hMSC (2×10^6) in two layers with 600 µm between the HUVEC cells. In vitro cultivation of bioprinted patches was reported, followed by in vivo transplantation of the cardiac patch into infarcted area of rat hearts after left anterior descending ligation. Eight weeks post transplantation, left ventricular catheterization was carried out to test cardiac patch performance. Results showed an increment in vessel formation, increased capillary density, and improvement in myocardial infracted heart functions [133].

Limitations of bioprinting

Though 3D bioprinting represents the hallmark innovative technology of this century, has led to numerous innovations in the medical field to improve human life quality, few limitations still prevail, which requires quick attention to make them a versatile tool.

Retaining the structure

Retaining structure accounts for the most commonly observed problem when printing bioinks as we encounter failure to maintain the exact shapes that were programmed. Post-printed 3D structures often collapses, swells, or dehydrates due to changes in temperature, humidity, pH, etc., affecting the overall quality and shows batch to batch variation.

Funding and budget issues

This undoubtedly remains the major challenge for the researchers worldwide as most commercial bioprinter shaves are fine-tuned for their respective bioinks, which further builds up the procurement cost. The majority of the high-quality, automated, and high-resolution bioprinters cost approx. $150 k–$200 k. Further, the development of in-house bioink and bioprinter remains a challenge that needs to be supported by various funding schemes.

Specific bioprinters

Among the various 3D bioprinters available in the market, most of them employ specific biocompatible materials and differ in their mechanism of action and may require variation in the nature of bioink (concentration, crosslinking mechanism, viscosity, etc.). Thus, all types of bioprinters do not bioprint similar 3D structures [134]

Compatible bioinks

The bioink forms the backbone of bioprinting and the type of bioprinter and the application of the 3D structure largely depends on the choice of bioinks. An ideal bioink helps in maintaining printability, formation of stable 3D structures, promotes cell growth and differentiation. Most of the hydrogel-based bioinks have been the ideal candidate material for cell encapsulation. The important parameters, including viscosity and shear thinning property of the hydrogel, hinders the printability and cell survival, while higher concentrations of hydrogels do not support cell viability and proliferation. Optimizing bioink for biomedical application requires strong scientific and technical knowledge, skilled labor, and time-consuming and expensive processes.

Choice of cells

The success of 3D printed structures depends on their ability to build viable 3D tissue constructs. The type of cells encapsulated into the bioinks commands the cell fate process and its ability to turn into various lineages. The use of live cells, including primary and stem cells, seems highly promising, but the availability and ethical issues restrict their utility. Robust use of stem cells and matching the application of bioprinting are reported by various researchers [135].

Design of 3D bioprinted structures

Literature reports successful printing of 3D structures following the software command of the bioprinter but still encounters the problem of vasculature needs focus. The pores and vasculature remain the deciding factors for nutrient transfer and oxygen supply. Apart from the constitution of bioinks, the size of the nozzle decides the pore size and thickness of the 3D structures. However, most of the currently available nozzles have large sizes that create void space and may lead to cell damage.

Validation of 3D bioprinted structure

Immense research studies support the proof of concept and report 3D bioprinted structure acceptable for organ regeneration and tablets for personalized medicine. But in reality, they

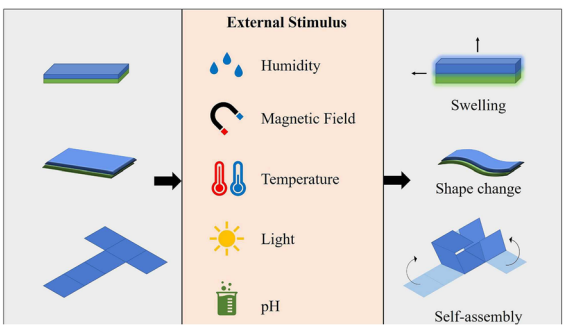

Figure 7: Types of stimuli in smart materials [reproduced from Ref. [137] open access Frontiers in Bioengineering and Biotechnology].

lack the actual formation of tissues to organ and still require extensive experiments or validation of these printed structures to take them to clinical trials.

Need for clinical translation

Despite enormous research and experimental data produced from 3D bioprinting, the clinical translations of this technology have been limited, and fewer animal studies and no potential 3D models in clinical trials make up the areas that need more focus [135, 136].

Four-dimensional (4D) printing

An extension and time-lapse method of 3D printing which demonstrates its ability to transform the 3D printed structure (still in printing bed) into function structure (without human intervention) by activation of heat, microwaves, pH, temperature, vibration, and light, or any other environmental stimuli form the 4D printing (Fig. 7). This technology was invented by researchers from the Massachusetts Institute of Technology, Self-Assembly Lab, and involves combining material programmability and engineering aspects.

Recently, Tamay and co-workers reviewed various factors that influence 4D printing viz., type of materials, stimulus exerted on 3D structure for transformation, the control mechanism for 3D to 4D conversion, material transformation property, and theoretical and numerical modeling/software—leading to shape shifting [137].

With tailor-made, scalable and smart materials, 4D printing could be a boon to the medical field. The cell viability could be controlled once the construct has been implanted into the human body and modified by body temperature, and this technology may be beneficial, for example, in the design of stents. The stent travels through the human body to a designated organ and could open up and aid in the theragnostic applications as well. Poly jet, selective laser melting and direct-write printing, the available systems for 4D printing, caters to biomedical applications. Figure 8 illustrates the variations in 3D and 4D printing. Various smart polymers used in 4D printing for tissue engineering applications have been discussed in the following sections.

Exploring 4D printing for biomedical applications

Ever since the advent of 3D bioprinting for medical application, the research focuses on developing functionalized organ in vitro. The concept is of 4D printing has uplifted and given a new focus for biomedical application. This system can effectively be utilized in healthcare sectors by understanding the human tissue dynamics and material kinetics. Integration of physiology and various branches of engineering can amazingly favor the strengthening of this new technology. The design of responsive materials scaffold fabrication is mandatory for any to kick starting the cellular activation. This stimulus is provided by smart polymers employed in 4D printing that can monitor tissue remodeling benefitting organ regeneration. Further, these materials hold potential as drug delivery vehicles that can imbibe the biological fluid when inserted in vivo and act on the target area/tissue by changing their release mechanism and behavior. The responsive stimulus can be based on temperature, pH, ionic concentration, enzyme activity that decides the drug release. These materials hold promising outcome when employed in tablet manufacturing. In the manufacture of medical devices including stent, lens, wound healing bandages, ligation paste, etc., the initial material's geometry with response behavior upon contact in the in vivo site leads to alteration in the dimensions of these implant materials for which the smart 4D printable materials are the strategic tools. The employability of these in medical diagnosis also holds

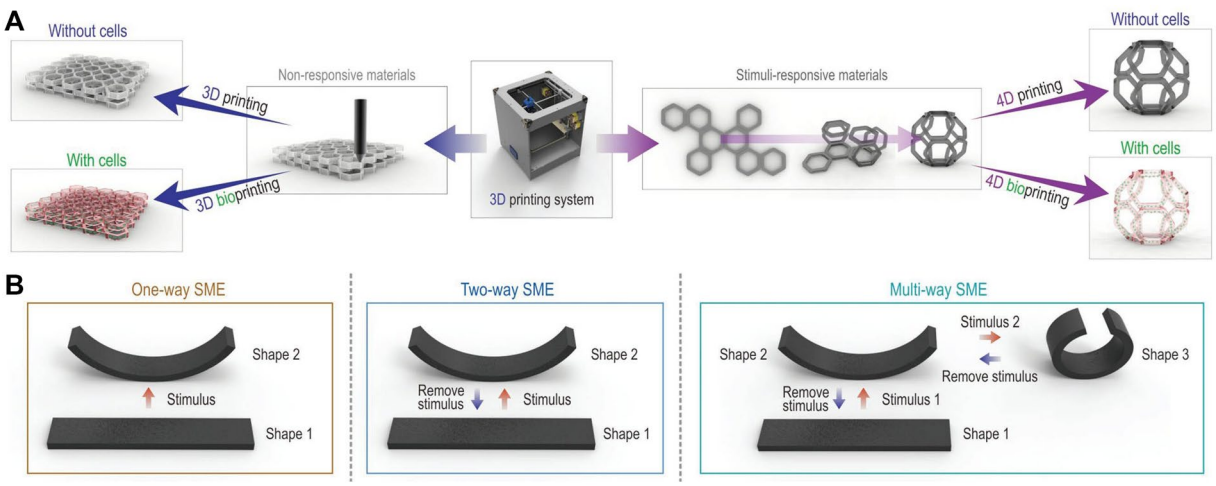

Figure 8: Schematics of 4D and 3D printing [reproduced with permission from Ref. [149] copyright with license Id: 51153702538000].

TABLE 4: 3D Vs 4D printing [reproduced from Ref. [137] open access Frontiers in Bioengineering and Biotechnology].

Property	3D Printing	4D printing
Manufacturing process printing	Layer by layer building of 3D structures (*x*, *y*, *z* axis)	Similar to 3D printing, while the shape of the material changes with response to external stimuli
Materials	Polymers, ceramics, metals, hydrogels, powders	Smart responsive materials that can change their dimension, shape, and function upon stimulus
Material Programming	Not possible	Can be programmed to various conditions including temperature, light, pH, electric & magnetic field
Stability	Stable with time and prone to degradation according to nature of the material	The material changes the shape upon stimulus and reverts back to original form when recovered
Application	Engineering, medicine, healthcare, manufacturing, production, etc	All areas of 3D printing where dynamics are required

promise. The careful selection of magneto and electric conductive polymers for sensing and scanning applications are other possibilities for utilizing smart materials in 4D printing. Table 4 shows the comparison between 3 and 4D bioprinting.

Regulatory issues

3D printing, a novel manufacturing methodology based on additive technique, has found wide applications in the biomedical field due to its immense potential to improve the treatment of different medical conditions. As discussed in previous sections, it has been employed in tissue engineering, disease modeling, and the diagnosis of various diseases. 3D printed drug product, i.e., Spritam® developed by Aprecia Pharmaceuticals has gained regulatory approval from the FDA for commercialization [138]. Considerable efforts are being devoted to use this versatile technology in various therapeutic strategies such as oral immediate release drug products, modified release preparations, and suppositories developed using 3D printing are at various stages of preclinical studies.

Additive manufacturing has allowed the development of material of any desired shape via printing materials through a layer-by-layer arrangement with the assistance of a 3D printer and developed complex structures using digital mode [139]. This novel technique allows high printing speed and can generate robust products with high reproducibility and low cost. Despite several advantages of this technique, various regulatory challenges have hampered its application. Current FDA guidelines do not govern 3D printers and regulate only biomedical products developed via additive manufacturing (i.e., raw materials, processes, and design software), which may pose a risk for patients [140]. Though FDA has approved different software programs for the fabrication of 3D models, it depends on the formulators to use them correctly for the intended use. Various medical devices developed by 3D printing and regulated by "FDA's Center for Devices and Radiological Health" classify into three categories depending upon the level of risk/regulatory control needed for developing safe and effective products; regulatory scrutiny increases from class I to class III devices. The devices with low risk (bandages), moderate risk (infusion pump), and high risk (life-supporting such as a pacemaker) fall under class I, II, and III, respectively. Class I and II devices do not undergo premarket review, but for class III, complete application submission for FDA review, including sufficient clinical trial data, appears mandatory. All devices need to comply with current good manufacturing practices to ensure the safety and quality of the final product. The FDA had issued a guideline in 2017 describing the information needed to develop 3D printed devices/implants. The guidance fails to address point-of-care manufacturing, presenting a gap between consistent and safe 3D printed models and various 3D printers taken by different hospitals [141].

Moreover, checking the clinical appropriateness of the products is still not covered under the scope of guidelines [142]. No proactive investigations have been carried out for products putting patients at risk, and state boards have taken care if any complaints were filed against any 3D printed product. Such significant problems have resulted from decentralized manufacturing of even high-risk products, including implants. Various 3D products being directly employed in clinical practices either for planning surgery or organ/tissue transplantation have made it difficult for the regulatory agency to categorize these as products or practices. The laws have not been fully imposed on them, putting patients at risk. Therefore, standardization should be carried out at hospitals/clinical sites considering patient safety as the foremost priority [143].

There were not been any specific guidance for the development of drugs and biological agents using 3D printing techniques by the FDA; the fabrication of these products regulates through the FDA's Centre for Drug Evaluation and Research and Centre for Biologics Evaluation and Research, respectively. The different guidelines for biological and non-biological agents could lead to complications for 3D products employing both in combination [140].

U.S. Food and Drug Organization has passed new guidelines in 2018 on "3D Printing of Medical Devices." *International*

Medical Device Regulators Forum also provided "Definitions for Personalized Medical Devices" in 2018 [144]. Moreover, *International Standardization Organization* and *American Society for Testing & Materials* have jointly framed the "Additive Manufacturing Standards Development Structure" aiming to identify gaps/needs and improvising usage and acceptance of 3D printed products [145]. The general standards including requirements/safety guidelines and standards for materials/processes involved in the development of 3D products have been framed. These guidelines will be very useful in implementation of standardized methodology for characterization of 3D printed products.

Future perspectives and conclusion

3D and next-generation 4D printing technologies have already become vital techniques for producing 3D structures for biomedical applications viz. organ regeneration, in vitro disease modeling, therapeutic implants, tablet manufacture, and sensor applications, which could be an answer for personalized medicine. Further, 3D printing via additive manufacturing has demonstrated usage in developing medical devices, surgical apparatus, and high-end equipment like ventilators. The limitations of material could be addressed by the printing technology owing to the availability of commercialized models for the various types of material used. The features like rapid speed, requirements of unskilled technicians, and minimum space make this technology the most sought-after one. Further from the clinical point of view, bench-to-bedside may be accomplished by 3D printing provided the laid down of specific regulatory issues, manufacturing guidelines, and quality control guidelines. 4D printing, a new branch of developing materials, has rapidly emerged as an innovation that requires the combined effort of material scientists, engineers, and medical professionals to come together and uplift the healthcare sector. In this review, we aimed to present the different facets of 3D and 4D printing and the outcomes of each are summarized in the respective sections. The detailed comparison between natural, synthetic, decellularized, and smart polymers for 3D and 4D printing points out the advantages and disadvantages of each polymers and their potential application in printing. This may in turn help the researchers to understand the purpose and choose the appropriate materials for successful 3D bioprinting. Further, the historical events related to the development of bioprinting and involvement of different bioprinters explaining their mechanistic behavior of the technique will pave way for choosing the appropriate instrument for printing process. In addition, the details of successfully 3D printed organs that support regeneration and development of tumor disease models using 3D printing are the varied arena of 3D bioprinting. The limitations of 3D bioprinting present the possible measures to overcome the failure of 3D structure and 4D printing as a new variant of 3D printing presents positive aspects by utilizing the dynamics and kinetics of the material. The current FDA guidelines for 3D printed products benefit the readers in understanding the complete process of printing till the product outcome.

Acknowledgments

The authors wish to acknowledge the Department of Science and Technology—Science Engineering Research Board, Early Career Research Award (ECR/2018/000709) for funding the research.

Declarations

Conflict of interest The authors declare that they have no known competing financial interests or personal relationships that could have appeared to influence the work reported in this paper.

Open Access

References

1. C. Mota, S. Camarero-Espinosa, M.B. Baker, P. Wieringa, L. Moroni, Bioprinting: from tissue and organ development to in vitro models. Chem. Rev. **120**, 10547–10607 (2020)
2. L.L. Wang, C.B. Highley, Y.C. Yeh, J.H. Galarraga, S. Uman, J.A. Burdick, Three- dimensional extrusion bioprinting of single and double network hydrogels containing dynamic covalent crosslinks. JBMR Part A. **106**, 865–875 (2018)
3. J. Vanderburgh, J.A. Sterling, S.A. Guelcher, 3D printing of tissue engineered constructs for in vitro modeling of disease progression and drug screening. Ann. Biomed. Eng. **45**, 164–179 (2017)

4. N. Ashammakhi, S. Ahadian, C. Xu, H. Montazerian, H. Ko, R. Nasiri, N. Barros, A. Khademhosseini, Bioinks and bioprinting technologies to make heterogeneous and biomimetic tissue constructs. Mater. Today Bio. **1**, 100008 (2019)
5. T. Tatsuaki, E. Ito, R. Kida, K. Hirose, T. Noda, T. Ozeki, 3D printing of gummy drug formulations composed of gelatin and an HPMC-based hydrogel for pediatric use. Int. J. Pharm. **594**, 120118 (2021)
6. W. Liu, Z. Zhong, N. Hu, Y. Zhou, L. Maggio, A.K. Miri, A. Fragasso, X. Jin, A. Khademhosseini, Y.S. Zhang, Coaxial extrusion bioprinting of 3D microfibrous constructs with cell-favorable gelatin methacryloyl microenvironments. Biofabrication. **10**, 024102 (2018)
7. P.S. Gungor-Ozkerim, I. Inci, Y.S. Zhang, A. Khademhosseini, M.R. Dokmeci, Bioinks for 3D bioprinting: an overview. Biomater. Sci. **6**, 915–946 (2018)
8. P. Jaipan, A. Nguyen, R.J. Narayan, Gelatin-based hydrogels for biomedical applications. Mrs Commun. **7**, 416–426 (2017)
9. B. Gozde, S.G. Ozcebe, B.W. Ellis, P. Zorlutuna, Tunable human myocardium derived decellularized extracellular matrix for 3D bioprinting and cardiac tissue engineering. Gels **7**, 70 (2021)
10. D. Chimene, K.K. Lennox, R.R. Kaunas, A.K. Gaharwar, Advanced bioinks for 3D printing: a materials science perspective. Ann. Biomed. Eng. **44**, 2090–2102 (2016)
11. S. Anil Kumar, M. Alonzo, S.C. Allen, L. Abelseth, V. Thakur, J. Akimoto, Y. Ito, S.M. Willerth, L. Suggs, M. Chattopadhyay, B. Joddar, A visible light-cross-linkable, fibrin–gelatin-based bioprinted construct with human cardiomyocytes and fibroblasts. ACS Biomater. Sci. Eng. **5**, 4551–4563 (2019)
12. K. Yue, G. Trujillo-de Santiago, M.M. Alvarez, A. Tamayol, N. Annabi, A. Khademhosseini, Synthesis, properties, and biomedical applications of gelatin methacryloyl (GelMA) hydrogels. Biomaterials **73**, 254–271 (2015)
13. W. Jia, P.S. Gungor-Ozkerim, Y.S. Zhang, K. Yue, K. Zhu, W. Liu, Q. Pi, B. Byambaa, M.R. Dokmeci, S.R. Shin, A. Khademhosseini, Direct 3D bioprinting of perfusable vascular constructs using a blend bioink. Biomaterials. **106**, 58–68 (2016)
14. G.A. Rico-Llanos, S. Borrego-González, M. Moncayo-Donoso, J. Becerra, R. Visser, Collagen type I biomaterials as scaffolds for bone tissue engineering. Polymers **13**, 599 (2021)
15. B. Claire, J. Chrenek, R.L. Kirsch, N.Z. Masri, H. Richards, K. Teetzen, S.M. Willerth, Natural biomaterials and their use as bioinks for printing tissues. Bioengineering **8**, 27 (2021)
16. S. Michael, H. Sorg, C.T. Peck, L. Koch, A. Deiwick, B. Chichkov, P.M. Vogt, K. Reimers, Tissue engineered skin substitutes created by laser-assisted bioprinting form skin-like structures in the dorsal skin fold chamber in mice. PloS ONE **8**, e57741 (2013)
17. V. Lee, G. Singh, J.P. Trasatti, C. Bjornsson, X. Xu, T.N. Tran, S.S. Yoo, G. Dai, P. Karande, Design and fabrication of human skin by three-dimensional bioprinting. Tissue Eng. Part C **20**, 473–484 (2014)
18. Z. Wu, X. Su, Y. Xu, B. Kong, W. Sun, S. Mi, Bioprinting three-dimensional cell-laden tissue constructs with controllable degradation. Sci. Rep. **6**, 1–10 (2016)
19. X. Yang, Z. Lu, H. Wu, W. Li, L. Zheng, J. Zhao, Collagen-alginate as bioink for three-dimensional (3D) cell printing based cartilage tissue engineering. Mater. Sci. Eng., C **83**, 195–201 (2018)
20. A. Francesca, X. Mu, S. Dirè, A. Motta, D.L. Kaplan, In situ 3D printing: opportunities with silk inks. Trends Biotechnol. **39**, 719–730 (2021)
21. N. Ruth, J. Ratanavaraporn, Mh.B. Fauzi, Comprehensive review of hybrid collagen and silk fibroin for cutaneous wound healing. Materials. **13**, 3097 (2020)
22. L.D. Koh, Y. Cheng, C.P. Teng, Y.W. Khin, X.J. Loh, S.Y. Tee, M. Low, E. Ye, H.D. Yu, Y.W. Zhang, M.Y. Han, Structures, mechanical properties and applications of silk fibroin materials. Prog. Polym. Sci. **46**, 86–110 (2015)
23. P. Admane, A.C. Gupta, P. Jois, S. Roy, C.C. Lakshmanan, G. Kalsi, B. Bandyopadhyay, S. Ghosh, Direct 3D bioprinted full-thickness skin constructs recapitulate regulatory signaling pathways and physiology of human skin. Bioprinting. **15**, e00051 (2019)
24. A. Sharma, G. Desando, M. Petretta, S. Chawla, I. Bartolotti, C. Manferdini, F. Paolella, E. Gabusi, D. Trucco, S. Ghosh, G. Lisignoli, Investigating the role of sustained calcium release in silk-gelatin-based three-dimensional bioprinted constructs for enhancing the osteogenic differentiation of human bone marrow derived mesenchymal stromal cells. ACS Biomater. Sci. Eng. **5**, 1518–1533 (2019)
25. K. Al, P. Tamer, S. Losi, G. Pierozzi, Soldani, A new method for fibrin-based electrospun/sprayed scaffold fabrication. Sci. Rep. **10**, 1–4 (2020)
26. F. Kreimendahl, C. Kniebs, A.M.T. Sobreiro, T. Schmitz-Rode, S. Jockenhoevel, A. Thiebes, FRESH bioprinting technology for tissue engineering - the influence of printing process and bioink composition on cell behavior and vascularization. J. Appl. Biomater. Funct. Mater. **19**, 22808000211028810 (2021)
27. S. England, A. Rajaram, D.J. Schreyer, X. Chen, Bioprinted fibrin-factor XIII-hyaluronate hydrogel scaffolds with encapsulated Schwann cells and their in vitro characterization for use in nerve regeneration. Bioprinting. **5**, 1–9 (2017)
28. J. Schöneberg, F. De Lorenzi, B. Theek, A. Blaeser, D. Rommel, A.J. Kuehne, F. Kießling, H. Fischer, Engineering biofunctional in vitro vessel models using a multilayer bioprinting technique. Sci. Rep. **8**, 1–13 (2018)

29. Z. Wang, S.J. Lee, H.J. Cheng, J.J. Yoo, A. Atala, 3D bioprinted functional and contractile cardiac tissue constructs. Acta Biomater. **70**, 48–56 (2018)
30. E. Pelin, I. Uvak, M.A. Nazeer, S.R. Batool, Y.N. Odeh, O. Akdogan, S. Kizilel, 3D Printing of cytocompatible gelatin-cellulose-alginate blend hydrogels. Macromol. Biosci. **20**, 2000106 (2020)
31. Y.J. Fan, H. Han-Yun, T. Sheng-Fang, W. Cheng-Hsuan, L. Chia-Ming, L. Yen-Ting, L. Chieh-Han, C. Shu-Wei, C. Bi-Chang, Microfluidic channel integrated with a lattice lightsheet microscopic system for continuous cell imaging. Lab Chip **21**, 344–354 (2021)
32. K. Christensen, C. Xu, W. Chai, Z. Zhang, J. Fu, Y. Huang, Freeform inkjet printing of cellular structures with bifurcations. Biotechnol. Bioeng. **112**, 1047–1055 (2015)
33. J.H. Shim, J.S. Lee, J.Y. Kim, D.W. Cho, Bioprinting of a mechanically enhanced three-dimensional dual cell-laden construct for osteochondral tissue engineering using a multi-head tissue/organ building system. J. Micromech. Microeng. **22**, 085014 (2012)
34. J. Gopinathan, I. Noh, Recent trends in bioinks for 3D printing. Biomater. Res. **22**, 1–15 (2018)
35. C.L. Carl Schuurmans, M. Mihajlovic, C. Hiemstra, K. Ito, W.E. Hennink, T. Vermonden, Hyaluronic acid and chondroitin sulfate (meth) acrylate-based hydrogels for tissue engineering: Synthesis, characteristics and pre-clinical evaluation. Biomaterials. **268**, 120602 (2021)
36. A. Gopal, S. Agiwal, A. Srivastava, Hyaluronic acid containing scaffolds ameliorate stem cell function for tissue repair and regeneration. Int. J. Biol. Macromol. **165**, 388–401 (2020)
37. J. Gopinathan, H.S. Shin, I.G. Kim, P. Ji, E.J. Chung, C. Lee, I. Noh, Self-crosslinking hyaluronic acid–carboxymethylcellulose hydrogel enhances multilayered 3D-printed construct shape integrity and mechanical stability for soft tissue engineering. Biofabrication **12**, 045026 (2020)
38. J.Y. Park, J.C. Choi, J.H. Shim, J.S. Lee, H. Park, S.W. Kim, J. Doh, D.W. Cho, A comparative study on collagen type I and hyaluronic acid dependent cell behavior for osteochondral tissue bioprinting. Biofabrication **6**, 035004 (2014)
39. G.F. Acosta-Vélez, C.S. Linsley, T.Z. Zhu, W. Wu, B.M. Wu, Photocurable bioinks for the 3D pharming of combination therapies. Polymers **10**, 1372 (2018)
40. B. Duan, E. Kapetanovic, L.A. Hockaday, J.T. Butcher, Three-dimensional printed trileaflet valve conduits using biological hydrogels and human valve interstitial cells. Acta Biomater. **10**, 1836–1846 (2014)
41. I. Noh, N. Kim, H.N. Tran, J. Lee, C. Lee, 3D printable hyaluronic acid-based hydrogel for its potential application as a bioink in tissue engineering. Biomater. Res. **23**, 1–9 (2019)
42. S. Li, X. Tian, J. Fan, H. Tong, Q. Ao, X. Wang, X, Chitosans for tissue repair and organ three-dimensional (3D) bioprinting. Micromachines. **10**, 765 (2019)
43. V.B. Morris, S. Nimbalkar, M. Younesi, P. McClellan, O. Akkus, Mechanical properties, cytocompatibility and manufacturability of chitosan: PEGDA hybrid-gel scaffolds by stereolithography. Ann. Biomed. Eng. **45**, 286–296 (2017)
44. T.H. Ang, F.S.A. Sultana, D.W. Hutmacher, Y.S. Wong, J.Y.H. Fuh, X.M. Mo, H.T. Loh, E. Burdet, S.H. Teoh, Fabrication of 3D chitosan–hydroxyapatite scaffolds using a robotic dispensing system. Mater. Sci. Eng., C **20**, 35–42 (2002)
45. Q. Gu, E. Tomaskovic Crook, R. Lozano, Y. Chen, R.M. Kapsa, Q. Zhou, G.G. Wallace, J.M. Crook, Functional 3D neural mini tissues from printed gel based bioink and human neural stem cells. Adv. Healthcare Mater. **5**, 1429–1438 (2016)
46. D.A. Taylor, L.C. Sampaio, Z. Ferdous, A.S. Gobin, L.J. Taite, Decellularized matrices in regenerative medicine. Acta Biomater. **74**, 74–89 (2018)
47. J.P. Jung, D.B. Bhuiyan, B.M. Ogle, Solid organ fabrication: comparison of decellularization to 3D bioprinting. Biomater. Res. **20**, 1–11 (2016)
48. F. Pati, J. Jang, D.H. Ha, S.W. Kim, J.W. Rhie, J.H. Shim, D.H. Kim, D.W. Cho, Printing three-dimensional tissue analogues with decellularized extracellular matrix bioink. Nat. Commun. **5**, 1–11 (2014)
49. M. Ali, A.K. Pr, J.J. Yoo, F. Zahran, A. Atala, S.J. Lee, A photocrosslinkable kidney ECM-derived bioink accelerates renal tissue formation. Adv. Healthcare Mater. **8**, 1800992 (2019)
50. B. Toprakhisar, A. Nadernezhad, E. Bakirci, N. Khani, G.A. Skvortsov, B. Koc, Development of bioink from decellularized tendon extracellular matrix for 3D bioprinting. Macromol. Biosci. **18**, 1800024 (2018)
51. W. Kim, G.H. Kim, An intestinal model with a finger-like villus structure fabricated using a bioprinting process and collagen/SIS-based cell-laden bioink. Theranostics. **10**, 2495 (2020)
52. W. Wu, A. DeConinck, J.A. Lewis, Omnidirectional printing of 3D microvascular networks. Adv. Mater. **23**, H178–H183 (2011)
53. E. Gioffredi, M. Boffito, S. Calzone, S.M. Giannitelli, A. Rainer, M. Trombetta, P. Mozetic, V. Chiono, Pluronic F127 hydrogel characterization and biofabrication in cellularized constructs for tissue engineering applications. Procedia Cirp. **49**, 125–132 (2016)
54. M. Müller, J. Becher, M. Schnabelrauch, M. Zenobi-Wong, Nanostructured Pluronic hydrogels as bioinks for 3D bioprinting. Biofabrication. **7**, 035006 (2015)
55. L. Roseti, C. Cavallo, G. Desando, V. Parisi, M. Petretta, I. Bartolotti, B. Grigolo, Three-dimensional bioprinting of cartilage by the use of stem cells: a strategy to improve regeneration. Materials. **11**, 1749 (2018)

56. M.J. Sawkins, P. Mistry, B.N. Brown, K.M. Shakesheff, L.J. Bonassar, J. Yang, Cell and protein compatible 3D bioprinting of mechanically strong constructs for bone repair. Biofabrication. **7**, 035004 (2015)
57. T. Guo, C.G. Lim, M. Noshin, J.P. Ringel, J.P. Fisher, 3D printing bioactive PLGA scaffolds using DMSO as a removable solvent. Bioprinting. **10**, 00038 (2018)
58. S. Zeng, J. Ye, Z. Cui, J. Si, Q. Wang, X. Wang, K. Peng, W. Chen, Surface biofunctionalization of three-dimensional porous poly (lactic acid) scaffold using chitosan/OGP coating for bone tissue engineering. Mater. Sci. Eng. C **77**, 92–101 (2017)
59. Y.W. Chen, Y.F. Shen, C.C. Ho, J. Yu, Y.H.A. Wu, K. Wang, C.T. Shih, M.Y. Shie, Osteogenic and angiogenic potentials of the cell-laden hydrogel/mussel-inspired calcium silicate complex hierarchical porous scaffold fabricated by 3D bioprinting. Mater. Sci. Eng. C **91**, 679–687 (2018)
60. J. Visser, F.P. Melchels, J.E. Jeon, E.M. Van Bussel, L.S. Kimpton, H.M. Byrne, W.J. Dhert, P.D. Dalton, D.W. Hutmacher, J. Malda, Reinforcement of hydrogels using three-dimensionally printed microfibres. Nat. Commun. **6**, 1–10 (2015)
61. W. Aljohani, M.W. Ullah, X. Zhang, G. Yang, Bioprinting and its applications in tissue engineering and regenerative medicine. Int. J. Biol. Macromol. **107**, 261–275 (2018)
62. T.K. Merceron, M. Burt, Y.J. Seol, H.W. Kang, S.J. Lee, J.J. Yoo, A. Atala, A 3D bioprinted complex structure for engineering the muscle–tendon unit. Biofabrication **7**, 035003 (2015)
63. F.Y. Hsieh, H.H. Lin, S.H. Hsu, 3D bioprinting of neural stem cell-laden thermoresponsive biodegradable polyurethane hydrogel and potential in central nervous system repair. Biomaterials **71**, 48–57 (2015)
64. H.H. Lin, F.Y. Hsieh, C.S. Tseng, S.H. Hsu, Preparation and characterization of a biodegradable polyurethane hydrogel and the hybrid gel with soy protein for 3D cell-laden bioprinting. J. Mater. Chem. B **4**, 6694–6705 (2016)
65. Q. Zou, B.E. Grottkau, Z. He, L. Shu, L. Yang, M. Ma, C. Ye, Biofabrication of valentine-shaped heart with a composite hydrogel and sacrificial material. Mater. Sci. Eng. C **108**, 110205 (2020)
66. K.S. Lim, R. Levato, P.F. Costa, M.D. Castilho, C.R. Alcala-Orozco, K.M. Van Dorenmalen, F.P. Melchels, D. Gawlitta, V.G.J. Hooper, J. Malda, T.B. Woodfield, Bio-resin for high resolution lithography-based biofabrication of complex cell-laden constructs. Biofabrication **10**, 034101 (2018)
67. F. Yu, X. Han, K. Zhang, B. Dai, S. Shen, X. Gao, H. Teng, X. Wang, L. Li, H. Ju, W. Wang, Evaluation of a polyvinyl alcohol-alginate based hydrogel for precise 3D bioprinting. JBMR Part A. **106**, 2944–2954 (2018)
68. R. Suntornnond, J. An, C.K. Chua, Bioprinting of thermoresponsive hydrogels for next generation tissue engineering: a review. Macromol. Mater. Eng. **302**, 1600266 (2017)
69. R. De Santis, U. D'Amora, T. Russo, A. Ronca, A. Gloria, L. Ambrosio, 3D fibre deposition and stereolithography techniques for the design of multifunctional nanocomposite magnetic scaffolds. JMSMM. **26**, 1–9 (2015)
70. S. Dutta, D. Cohn, Temperature and pH responsive 3D printed scaffolds. J. Mater. Chem. B **48**, 9514–9521 (2017)
71. K. Sumaru, K. Ohi, T. Takagi, T. Kanamori, T. Shinbo, Photoresponsive properties of poly (N-isopropylacrylamide) hydrogel partly modified with spirobenzopyran. Langmuir **22**, 4353–4356 (2006)
72. F. Pati, J. Jang, J.W. Lee, D.W. Cho, Extrusion bioprinting, in *Essentials of 3D biofabrication and translation*. ed. by A. Atala, J.J. Yoo (Academic Press, London, 2015)
73. I. Apsite, G. Stoychev, W. Zhang, D. Jehnichen, J. Xie, L. Ionov, Porous stimuli-responsive self-folding electrospun mats for 4D biofabrication. Biomacromol **18**, 3178–3184 (2017)
74. X. Liu, K. Zhao, T. Gong, J. Song, C. Bao, E. Luo, J. Weng, S. Zhou, Delivery of growth factors using a smart porous nanocomposite scaffold to repair a mandibular bone defect. Biomacromol **15**, 1019–1030 (2014)
75. D. Zhou, J. Chen, B. Liu, X. Zhang, X. Li, T. Xu, Bioinks for jet-based bioprinting. Bioprinting. **16**, 00060 (2019)
76. C. Ru, J. Luo, S. Xie, Y. Sun, A review of non-contact micro- and nano-printing technologies. J. Micromech. Microeng. **24**, 053001 (2014)
77. U. Jammalamadaka, K. Tappa, Recent advances in biomaterials for 3D printing and tissue engineering. J. Funct. Biomater. **9**, 22 (2018)
78. E. Tekin, P.J. Smith, U.S. Schubert, Inkjet printing as a deposition and patterning tool for polymers and inorganic particles. Soft Matter **4**, 703–713 (2008)
79. S. Vijayavenkataraman, W.C. Yan, W.F. Lu, C.H. Wang, J.Y.H. Fuh, 3D bioprinting of tissues and organs for regenerative medicine. Adv. Drug Deliv. Rev. **132**, 296–332 (2018)
80. T. Xu, W. Zhao, J.M. Zhu, M.Z. Albanna, J.J. Yoo, A. Atala, Complex heterogeneous tissue constructs containing multiple cell types prepared by inkjet printing technology. Biomaterials **34**, 130–139 (2013)
81. U. Demirci, G. Montesano, Single cell epitaxy by acoustic picolitre droplets. Lab Chip **7**, 1139–1145 (2007)
82. W.L. Ng, J.M. Lee, W.Y. Yeong, M.W. Naing, Microvalve-based bioprinting–process, bio-inks and applications. Biomater. Sci. **5**, 632–647 (2017)
83. L. Horváth, Y. Umehara, C. Jud, F. Blank, A. Petri-Fink, B. Rothen-Rutishauser, Engineering an in vitro air-blood barrier by 3D bioprinting. Sci. Rep. **5**, 1–8 (2015)
84. V.K. Lee, A.M. Lanzi, H. Ngo, S.S. Yoo, P.A. Vincent, G. Dai, Generation of multi-scale vascular network system within 3D hydrogel using 3D bio-printing technology. Cell. Mol. Bioeng. **7**, 460–472 (2014)

85. M.S. Onses, E. Sutanto, P.M. Ferreira, A.G. Alleyne, J.A. Rogers, Mechanisms, capabilities, and applications of high resolution electrohydrodynamic jet printing. Small **11**, 237–4266 (2015)
86. J.U. Park, J.H. Lee, U. Paik, Y. Lu, J.A. Rogers, Nanoscale patterns of oligonucleotides formed by electrohydrodynamic jet printing with applications in biosensing and nanomaterials assembly. Nano Lett. **8**, 4210–4216 (2008)
87. S. Vijayavenkataraman, S. Thaharah, S. Zhang, W.F. Lu, J.Y.H. Fuh, Electrohydrodynamic jet 3D-printed PCL/PAA conductive scaffolds with tunable biodegradability as nerve guide conduits (NGCs) for peripheral nerve injury repair. Mater. Des. **162**, 171–184 (2019)
88. P. Sasmal, P. Datta, Y. Wu, I.T. Ozbolat, 3D bioprinting for modelling vasculature. Microphysiol. Syst. **1**, 1 (2018)
89. R. Bhuthalingam, P.Q. Lim, S.A. Irvine, A. Agrawal, P.S. Mhaisalkar, J. An, C.K. Chua, S. Venkatraman, A novel 3D printing method for cell alignment and differentiation. Int. J. Bioprint. (2015). https://doi.org/10.18063/IJB.2015.01.008
90. F.P. Melchels, M.A. Domingos, T.J. Klein, J. Malda, P.J. Bartolo, D.W. Hutmacher, Additive manufacturing of tissues and organs. Prog. Polym. Sci. **37**, 1079–1104 (2012)
91. S. Ji, E. Almeida, M. Guvendiren, 3D bioprinting of complex channels within cell-laden hydrogels. Acta Biomater. **95**, 214–224 (2019)
92. N.T. Raveendran, C. Vaquette, C. Meinert, D.S. Ipe, S. Ivanovski, Optimization of 3D bioprinting of periodontal ligament cells. Dent. Mater. **35**, 683–1694 (2019)
93. C. Mandrycky, Z. Wang, K. Kim, D.H. Kim, 3D bioprinting for engineering complex tissues. Biotechnol. Adv. **34**, 422–434 (2016)
94. M.D. Sarker, S. Naghieh, N.K. Sharma, X. Chen, 3D biofabrication of vascular networks for tissue regeneration: a report on recent advances. J. Pharm. Anal. **8**, 277–296 (2018)
95. D. Zhang, J. Zhou, X. Chen, X. Zhang, W. Li, T. Zhao, Xu, Biomaterials based on marine resources for 3D bioprinting applications. Mar. Drugs **17**, 555 (2019)
96. J.R. Tumbleston, D. Shirvanyants, N. Ermoshkin, R. Januszewicz, A.R. Johnson, D. Kelly, K. Chen, R. Pinschmidt, J.P. Rolland, A. Ermoshkin, E.T. Samulski, Continuous liquid interface production of 3D objects. Science **347**, 1349–1352 (2015)
97. C. Yu, X. Ma, W. Zhu, P. Wang, K.L. Miller, J. Stupin, A. Koroleva-Maharajh, A. Hairabedian, S. Chen, Scanningless and continuous 3D bioprinting of human tissues with decellularized extracellular matrix. Biomaterials **194**, 1–13 (2019)
98. Y. Zhang, Y. Yu, I.T. Ozbolat, Direct bioprinting of vessel-like tubular microfluidic channels. J. Nanotechnol. Eng. Med. **4**, 020902 (2013)
99. J. Schöneberg, F. De Lorenzi, B. Theek, A. Blaeser, D. Rommel, A.J. Kuehne, F. Kießling, H. Fischer, Engineering biofunctional in vitro vessel models using a multilayer bioprinting technique. Sci. Rep. **8**, 1–13 (2018)
100. Y. Nishiyama, M. Nakamura, C. Henmi, K. Yamaguchi, S. Mochizuki, H. Nakagawa, K. Takiura, Development of a three-dimensional bioprinter: construction of cell supporting structures using hydrogel and state-of-the-art inkjet technology. J. Biomech. Eng. **131**, 035001 (2009)
101. J.M. Bourget, O. Kérourédan, M. Medina, M. Rémy, N.B. Tzhébaud, R. Bareille, O. Chassande, J. Amédée, S. Catros, R. Devillard, Patterning of endothelial cells and mesenchymal stem cells by laser-assisted bioprinting to study cell migration. BioMed Res. Int. **2016**, 1–7 (2016)
102. L.K. Narayanan, P. Huebner, M.B. Fisher, J.T. Spang, B. Starly, R.A. Shirwaiker, 3D-bioprinting of polylactic acid (PLA) nanofiber–alginate hydrogel bioink containing human adipose-derived stem cells. ACS Biomater. Sci. Eng. **2**, 1732–1742 (2016)
103. S.T. Bendtsen, S.P. Quinnell, M. Wei, Development of a novel alginate-polyvinyl alcohol-hydroxyapatite hydrogel for 3D bioprinting bone tissue engineered scaffolds. JBMR Part A. **105**, 1457–1468 (2017)
104. G. Gao, A.F. Schilling, T. Yonezawa, J. Wang, G. Dai, X. Cui, Bioactive nanoparticles stimulate bone tissue formation in bioprinted three-dimensional scaffold and human mesenchymal stem cells. Biotechnol. J. **9**, 1304–1311 (2014)
105. B. Byambaa, N. Annabi, K. Yue, G. Trujillo-de Santiago, M.M. Alvarez, W. Jia, M. Kazemzadeh-Narbat, S.R. Shin, A. Tamayol, A. Khademhosseini, Bioprinted osteogenic and vasculogenic patterns for engineering 3D bone tissue. Adva. Healthcare Mater. **6**, 1700015 (2017)
106. A. Wenz, K. Borchers, G.E. Tovar, P.J. Kluger, Bone matrix production in hydroxyapatite-modified hydrogels suitable for bone bioprinting. Biofabrication **9**, 044103 (2017)
107. V. Keriquel, H. Oliveira, M. Rémy, S. Ziane, S. Delmond, B. Rousseau, S. Rey, S. Catros, J. Amédée, F. Guillemot, J.C. Fricain, In situ printing of mesenchymal stromal cells, by laser-assisted bioprinting, for in vivo bone regeneration applications. Sci. Rep. **7**, 1–10 (2017)
108. V.H. Mouser, R. Levato, L.J. Bonassar, D.D. D'Lima, D.A. Grande, T.J. Klein, D.B. Saris, M. Zenobi-Wong, D. Gawlitta, J. Malda, Three-dimensional bioprinting and its potential in the field of articular cartilage regeneration. Cartilage. **8**, 327–340 (2017)
109. S.W. Kim, D.Y. Kim, H.H. Roh, H.S. Kim, J.W. Lee, K.Y. Lee, Three-dimensional bioprinting of cell-laden constructs using polysaccharide-based self-healing hydrogels. Biomacromol **20**, 1860–1866 (2019)
110. M. Gruene, A. Deiwick, L. Koch, S. Schlie, C. Unger, N. Hofmann, I. Bernemann, B. Glasmacher, B. Chichkov, Laser printing of stem cells for biofabrication of scaffold-free autologous grafts. Tissue Eng. Part C Methods **17**, 79–87 (2011)
111. T. Xu, K.W. Binder, M.Z. Albanna, D. Dice, W. Zhao, J.J. Yoo, A. Atala, Hybrid printing of mechanically and biologically improved constructs for cartilage tissue engineering applications. Biofabrication **5**, e015001 (2012)

112. S. Rhee, J.L. Puetzer, B.N. Mason, C.A. Reinhart-King, L.J. Bonassar, 3D bioprinting of spatially heterogeneous collagen constructs for cartilage tissue engineering. ACS Biomater. Sci. Eng. **2**, 1800–1805 (2016)
113. M.N. Hirt, A. Hansen, T. Eschenhagen, Cardiac tissue engineering: state of the art. Circ. Res. **114**, 354–367 (2014)
114. K. Jakab, C. Norotte, B. Damon, F. Marga, A. Neagu, C.L. Besch-Williford, A. Kachurin, K.H. Church, H. Park, V. Mironov, R. Markwald, Tissue engineering by self-assembly of cells printed into topologically defined structures. Tissue Eng. Part A **14**, 413–421 (2008)
115. F. Maiullari, M. Costantini, M. Milan, V. Pace, M. Chirivì, S. Maiullari, A. Rainer, D. Baci, H.E.S. Marei, D. Seliktar, C. Gargioli, A multi-cellular 3D bioprinting approach for vascularized heart tissue engineering based on HUVECs and iPSC-derived cardiomyocytes. Sci. Rep. **8**, 1–15 (2018)
116. Y.S. Zhang, A. Arneri, S. Bersini, S.R. Shin, K. Zhu, Z. Goli-Malekabadi, J. Aleman, C. Colosi, F. Busignani, V. Dell'Erba, C. Bishop, Bioprinting 3D microfibrous scaffolds for engineering endothelialized myocardium and heart-on-a-chip. Biomaterials **110**, 45–59 (2016)
117. C. Kryou, V. Leva, M. Chatzipetrou, I. Zergioti, Bioprinting for liver transplantation. Bioengineering **6**, 95 (2019)
118. Y. Kim, K. Kang, J. Jeong, S.S. Paik, J.S. Kim, S.A. Park, W.D. Kim, J. Park, D. Choi, Three-dimensional (3D) printing of mouse primary hepatocytes to generate 3D hepatic structure. Ann. Surg. Treat. Res. **92**, 67 (2017)
119. A. Faulkner-Jones, C. Fyfe, D.J. Cornelissen, J. Gardner, J. King, A. Courtney, W. Shu, Bioprinting of human pluripotent stem cells and their directed differentiation into hepatocyte-like cells for the generation of mini-livers in 3D. Biofabrication. **7**, 044102 (2015)
120. Y. Wu, Z.Y.W. Lin, A.C. Wenger, K.C. Tam, X.S. Tang, 3D bioprinting of liver-mimetic construct with alginate/cellulose nanocrystal hybrid bioink. Bioprinting. **9**, 1–6 (2018)
121. L. Koch, S. Kuhn, H. Sorg, M. Gruene, S. Schlie, R. Gaebel, B. Polchow, K. Reimers, S. Stoelting, N. Ma, P.M. Vogt, Laser printing of skin cells and human stem cells. Tissue Eng. Part C Methods **16**, 847–854 (2010)
122. W. Lee, J.C. Debasitis, V.K. Lee, J.H. Lee, K. Fischer, K. Edminster, J.K. Park, S.S. Yoo, Multi-layered culture of human skin fibroblasts and keratinocytes through three-dimensional free form fabrication. Biomaterials **30**, 1587–1595 (2009)
123. M. Yanez, J. Rincon, A. Dones, C. De Maria, R. Gonzales, T. Boland, In vivo assessment of printed microvasculature in a bilayer skin graft to treat full-thickness wounds. Tissue Eng. Part A **21**, 224–233 (2015)
124. L.J. Pourchet, A. Thepot, M. Albouy, E.J. Courtial, A. Boher, L.J. Blum, C.A. Marquette, Human skin 3D bioprinting using scaffold free approach. Adv. Healthcare Mater. **6**, 1601101 (2017)
125. S. Knowlton, S. Onal, C.H. Yu, J.J. Zhao, S. Tasoglu, Bioprinting for cancer research. Trends Biotechnol. **33**, 504–513 (2015)
126. F. Xu, J. Celli, I. Rizvi, S. Moon, T. Hasan, U. Demirci, A three dimensional in vitro ovarian cancer coculture model using a high throughput cell patterning platform. Biotechnol. J. **6**, 204–212 (2011)
127. Y. Zhao, R. Yao, L. Ouyang, H. Ding, T. Zhang, K. Zhang, S. Cheng, W. Sun, Three-dimensional printing of Hela cells for cervical tumor model in vitro. Biofabrication. **6**, 035001 (2014)
128. T.Q. Huang, X. Qu, J. Liu, S. Chen, 3D printing of biomimetic microstructures for cancer cell migration. Biomed. Microdevice **16**, 127–132 (2014)
129. X. Dai, C. Ma, Q. Lan, T. Xu, 3D bioprinted glioma stem cells for brain tumor model and applications of drug susceptibility. Biofabrication **8**, 045005 (2016)
130. S. Swaminathan, Q. Hamid, W. Sun, A.M. Clyne, Bioprinting of 3D breast epithelial spheroids for human cancer models. Biofabrication **11**, e025003 (2019)
131. D. Bejleri, B.W. Streeter, A.L. Nachlas, M.E. Brown, R. Gaetani, K.L. Christman, M.E. Davis, A bioprinted cardiac patch composed of cardiac-specific extracellular matrix and progenitor cells for heart repair. Adv. Healthcare Mater. **7**, 1800672 (2018)
132. M.S. Rahman, M.M. Rana, L.S. Spitzhorn, N. Akhtar, M.Z. Hasan, N. Choudhury, T. Fehm, J.T. Czernuszka, J. Adjaye, S.M. Asaduzzaman, Fabrication of biocompatible porous scaffolds based on hydroxyapatite/collagen/chitosan composite for restoration of defected maxillofacial mandible bone. Prog. Biomater. **8**, 137–154 (2019)
133. R. Gaebel, N. Ma, J. Liu, J. Guan, L. Koch, C. Klopsch, M. Gruene, A. Toelk, W. Wang, P. Mark, F. Wang, Patterning human stem cells and endothelial cells with laser printing for cardiac regeneration. Biomaterials **32**, 9218–9230 (2011)
134. F. Zhao, J. Wang, H. Guo, S. Liu, W. He, The effects of surface properties of nanostructured bone repair materials on their performances. J. Nanomater. **2015**, 1–11 (2015)
135. M.A. Heinrich, W. Liu, A. Jimenez, J. Yang, A. Akpek, X. Liu, Q. Pi, X. Mu, N. Hu, R.M. Schiffelers, J. Prakash, 3D bioprinting: from benches to translational applications. Small **15**, 1805510 (2019)
136. D. Stanco, P. Urbán, S. Tirendi, G. Ciardelli, J. Barrero, 3D bioprinting for orthopaedic applications: Current advances, challenges and regulatory considerations. Bioprinting **20**, 100103 (2020)
137. D.G. Tamay, T. Dursun Usal, A.S. Alagoz, D. Yucel, N. Hasirci, V. Hasirci, 3D and 4D printing of polymers for tissue engineering applications. Front. Bioeng. Biotechnol. **7**, 164 (2019)
138. Aprecia. Spritam 2015 [Available from: https://www.aprecia.com/zipdoseplatform/zipdose-technology.php.
139. W.L. Ng, C.K. Chua, Y.F. Shen, Print me an organ! Why we are not there yet. Progress Polym. Sci. **97**, 101145 (2019)

140. M. Di Prima, J. Coburn, D. Hwang, J. Kelly, A. Khairuzzaman, L. Ricles, Additively manufactured medical products–the FDA perspective. 3D Print. Med. **2**, 1–6 (2016)
141. Regulation (EU) 2017/745 of the European Parliament and of the Council of 5 April 2017 on Medical Devices. 2017
142. A. Horst, F. McDonald, Uncertain but not unregulated: medical product regulation in the light of three-dimensional printed medical products. 3D Print. Addit. Manuf. **7**, 248–257 (2020)
143. A. Christensen, F.J. Rybicki, Maintaining safety and efficacy for 3D printing in medicine. 3D Print. Med. **3**, 1–10 (2017)
144. J.C. Schuh, K.A. Funk, Compilation of international standards and regulatory guidance documents for evaluation of biomaterials, medical devices, and 3-D printed and regenerative medicine products. Toxicol. Pathol. **47**(3), 344–357 (2019)
145. D. Stanco, P. Urbán, S. Tirendi, G. Ciardelli, J. Barrero, 3D bioprinting for orthopaedic applications: Current advances, challenges and regulatory considerations. Bioprinting. **23**, 100103 (2020)
146. Y. Zhang, L. Huang, H. Song, C. Ni, J. Wu, Q. Zhao, T. Xie, 4D printing of a digital shape memory polymer with tunable high performance. ACS Appl. Mater. Interfaces. **11**, 32408–32413 (2019)
147. Y. Mao, K. Yu, M.S. Isakov, J. Wu, M.L. Dunn, H.J. Qi, Sequential self-folding structures by 3D printed digital shape memory polymers. Sci. Rep. **5**, 1–12 (2015)
148. J.G. Fisher, E.A. Sparks, F.A. Khan, B. Dionigi, H. Wu, J. Brazzo III., D. Fauza, B. Modi, D.L. Safranski, T. Jaksic, Extraluminal distraction enterogenesis using shape-memory polymer. J. Pediatr. Surg. **50**, 938–942 (2015)
149. G.H. Yang, M. Yeo, Y.W. Koo, G.H. Kim, 4D bioprinting: technological advances in biofabrication. Macromol. Biosci. **19**, 1800441 (2019)